

INFORMATION TO USERS

This reproduction was made from a copy of a manuscript sent to us for publication and microfilming. While the most advanced technology has been used to photograph and reproduce this manuscript, the quality of the reproduction is heavily dependent upon the quality of the material submitted. Pages in any manuscript may have indistinct print. In all cases the best available copy has been filmed.

The following explanation of techniques is provided to help clarify notations which may appear on this reproduction.

1. Manuscripts may not always be complete. When it is not possible to obtain missing pages, a note appears to indicate this.
2. When copyrighted materials are removed from the manuscript, a note appears to indicate this.
3. Oversize materials (maps, drawings, and charts) are photographed by sectioning the original, beginning at the upper left hand corner and continuing from left to right in equal sections with small overlaps. Each oversize page is also filmed as one exposure and is available, for an additional charge, as a standard 35mm slide or in black and white paper format.*
4. Most photographs reproduce acceptably on positive microfilm or microfiche but lack clarity on xerographic copies made from the microfilm. For an additional charge, all photographs are available in black and white standard 35mm slide format.*

*For more information about black and white slides or enlarged paper reproductions, please contact the Dissertations Customer Services Department.

UMI University
Microfilms
International

8614671

El-Hefnawi, Sobhy Abdel Hamid

**ELECTRON SPIN RESONANCE STUDIES OF THE STRUCTURE OF
TRIARYLTIN RADICALS**

City University of New York

PH.D. 1986

**University
Microfilms
International** 300 N. Zeeb Road, Ann Arbor, MI 48106

Copyright 1986

by

El-Hefnawi, Sobhy Abdel Hamid

All Rights Reserved

**ELECTRON SPIN RESONANCE STUDIES
OF THE STRUCTURE OF TRIARYLTIN
RADICALS**

by

SOBHY ABDEL HAMID EL-HEFNAWI

**A dissertation submitted to the Graduate Faculty in
Chemistry in partial fulfillment of the requirements
for the degree of Doctor of Philosophy,
The City University of New York.**

1986

© 1986

SOBHY ABDEL HAMID EL-HEFNAWI

All Rights Reserved

This manuscript has been read and accepted for the Graduate Faculty in Chemistry in satisfaction of the dissertation requirement for the degree of Doctor of Philosophy.

4/28/86
Date

H. Brannock
Chair of Examining Committee

4/29/86
Date

A. M. [Signature]
Executive Officer

Evan T. Williams
Evan T. Williams

Nan-Loh Yang
Nan-Loh Yang

Supervisory Committee

The City University of New York

ABSTRACT

ELECTRON SPIN RESONANCE STUDIES OF THE STRUCTURE OF TRIARYLTIN RADICALS

by

Sobhy Abdel Hamid El-Hefnawi

Advisor: Professor Fitzgerald B. Bramwell

Electron spin resonance (ESR) spectra of isotopically enriched (^{119}Sn) triphenyltin, triparatolytin and triorthotolytin radicals in rigid glass solution are reported at 4 K and 93 K. Radicals were generated by visible light photo-oxidation of triaryltin anions. Anions were synthesized by alkali metal reduction of tetryltin in 2-methyltetrahydrofuran.

The isotropic and anisotropic hyperfine splitting have been determined using the Breit-Rabi equation. From this data we have used a semi-empirical approach to estimate the "S" and "P" character of the orbital containing the unpaired electron, the extent of hybridization, the ligand-tin-ligand bond angle, $\bar{\alpha}$, and the ligand-symmetry axis complementary angle, θ , (out-of-plane bond angle).

From an analyses of the spectra the, following conclusions were drawn: triphenyltin and triparatolytin radicals appear to be relatively stable, pyramidal structures with ligand-tin-ligand bond angles of 114.6° , and 114.8° , respectively. Ligand-symmetry axis complementary angles are 13.6° , 13.4° , respectively.

Triorthotolytin radical appears to have a deeper pyramidal structure with a ligand-tin-ligand bond angle of 114.4° and a ligand-symmetry axis complementary angle of 13.9° . These results are discussed in terms of limited tin-carbon multiple bonding and in terms of steric effects.

DEDICATED

**TO
MY WIFE
AND
MY PARENTS**

ACKNOWLEDGMENTS

I wish to express my gratitude to Nilda, my wife, for typing the manuscript, and for her patience, support and encouragement throughout my studies. I am also deeply indebted to Professor F. B. Brawwell, of Brooklyn College, for his invaluable assistance in and out of the laboratory and for his editing and correcting the manuscript.

I also should like to thank Professor N-L Yang, of Staten Island College; Professor E. Williams, and Professor C. Dillard, of Brooklyn College, for their helpful discussions and encouragement.

My gratitude extends to all my friends in the Chemistry Department at Brooklyn College. It is a pleasure to acknowledge the skillful and timely glassware work of Mr. Ottmar Safferling, who fabricated most of my glass equipment and made numerous quick repairs.

Finally I wish to thank Ronald Soto for his suggestions and his computer knowledge.

TABLE OF CONTENTS

	Page
ABSTRACT.....	iv
ACKNOWLEDGEMENTS.....	vii
LIST OF TABLES.....	x
LIST OF ILLUSTRATIONS.....	xi
 CHAPTER	
I. INTRODUCTION.....	1
II. GENERAL THEORETICAL CONSIDERATIONS.....	5
II. A. \hat{H}_Z - The Electronic Zeeman Effect.....	6
II. B. \hat{H}_H - Hyperfine Coupling.....	14
1. Anisotropic Hyperfine Coupling....	14
2. Isotropic Hyperfine Coupling.....	18
3. The Breit-Rabi Equation.....	19
II. C. \hat{H}_N - The Nuclear Zeeman Interaction...	22
II. D. Spectral Analysis.....	23
III. EXPERIMENTAL	28
III. A. SYNTHESIS.....	28
Preparation of:	
Metallic Tin.....	28
Stannic Iodide.....	29
Tetraphenyltin.....	31
Triphenyltin Chloride.....	34
Triphenyl-1-Cyclopentadienyltin...	36
Triphenyltin Hydride.....	40
Tetrakisparatolytin.....	42
Trisparatolytin Bromide.....	44
Trisparatolytin Hydride.....	46
Tetrakisorthotolytin.....	48
Trisorthotolytin Bromide.....	51
Trisorthotolytin Hydride.....	53
Tetrakismetatolytin.....	55
Trismetatolytin Chloride.....	58
Trismetatolytin Hydride.....	60

Chapter	Page
III. B. TECHNIQUES.....	62
1. ESR Spectrometer.....	62
2. The ESR Cold Temperature Cell.....	62
3. Purification of Solvent.....	63
4. Light Source.....	64
5. Sample Preparation.....	65
a. Sodium-potassium Experiments.	65
b. t-Butyl Peroxide Experiments.	73
c. Cyclopentadienyl Experiments.	74
IV. RESULTS.....	75
IV. A. Tetraphenyltin.....	75
IV. B. Tetrakisparatolytin.....	96
IV. C. Tetrakisorthotolytin.....	111
IV. D. t-Butyl Peroxide.....	126
IV. E. Cyclopentadienyl.....	128
V. DISCUSSION.....	129
APPENDIX.....	133
A. Computer Programs.....	133
I. Theoretical Calculation of Triaryltin Compounds.....	133
II. Theoretical Calculation of Low-Field Satellite Position.....	137
III. Theoretical Calculation of Hyperfine Splitting.....	139
BIBLIOGRAPHY.....	141

LIST OF TABLES

Table		Page
1.	Hyperfine Splitting and g-Factor Parameters for Triphenyltin Radical.....	91
2.	The ESR Parameters for Triaryltin Radicals.....	92
3.	"S" and "P" Character of the Central Atom for Triphenyltin Radical in 2-MTHF at 93 K.....	93
4.	Observed and Calculated Triaryltin Radical ESR Line Position.....	95

LIST OF ILLUSTRATIONS

Figure	Page
1. The Distribution of g and g in a Randomly Oriented Sample with a Threefold or Higher Axis.	11
2. Absorbtion Line Shape for Axial Symmetry with g -Factor Anisotropy.....	13
3. Powder ESR Spectrum for Hypothetical Radical with $S = \frac{1}{2}$, $I = \frac{1}{2}$ and Axial Symmetry.....	27
4A. A Schematic Diagram of a Reaction Vessel.....	68
4B. A Schematic Diagram of a Reaction Vessel Under the Vacuum Line.....	70
4C. The Reaction Vessel Removed from the Vacuum Line	72
5. NMR Spectrum of Triphenyltin Anion in 2-MTHF....	77
6. The ESR Spectra of Triphenyltin Radical in 2-MTHF at 93 K.....	80
6A. Base Line - Sample in Place but not Irradiated..	80
6B. Visible Light Irradiation of the Sample.....	80
6C. UV Light Irradiation of the Sample.....	90
7. The ESR Spectra of the Central Signal of Triphenyltin Radical in 2-MTHF at 93 K.....	84
8. NMR Spectrum of Triparatolytin Anion in 2-MTHF.	98
9. The ESR Spectra of Triparatolytin Radical in 2-MTHF at 93 K.....	102
9A. Base Line - Sample in Place but not Irradiated..	102
9B. Visible Light Irradiation of the Sample.....	102
9C. UV Light Irradiation of the Sample.....	110

Figure	Page
10. The ESR Spectra of the Central Signal of Tri- paratolytin Radical in 2-MTHF at 93 K.....	105
11. NMR Spectrum of Triorthotolytin Anion in 2-MTHF	113
12. The ESR Spectra of Triorthotolytin Radical in 2-MTHF at 93 K.....	116
12A. Base Line - Sample in Place but not Irradiated..	116
12B. Visible Light Irradiation of the Sample.....	116
12C. UV Light Irradiation of the Sample.....	125
13. The ESR Spectra of the Central Signal of Tri- orthotolytin Radical in 2-MTHF at 93 K.....	119

I. INTRODUCTION

The structure of triaryltin radicals is of considerable interest because of the possibility of tin-ligand multiple bonding through the interaction of low lying tin d-orbitals with ligand pi-orbitals. Although extensive electron spin resonance (ESR) studies of alkyl tin radicals have been made, there have been relatively few observations of aryltin radicals. The results of aryltin radical experiments have not led to a consistent picture of the structure, extent, and type of bonding present in such compounds.

Gordy and co-workers (1) have shown that a decrease in g value is expected with increasing "S" character of the free electron orbital in radicals with atoms exhibiting appreciable spin-orbit coupling. While trialkyl tin radicals R_3Sn ($R = Me, n-Pr, n-Bu$), appear to have a relatively pyramidal structure (2, 3), the decrease in the g values in the series $R_3Sn, R_2PhSn, RPh_2Sn, Ph_3Sn$ ($R = Me, Et$) indicates increasing pyramidal character. A change in the geometry of the radicals is assumed to be the reason for the decreasing g values.

The conclusion of these studies was that the greater the number of phenyl substituents, the more pyramidal the radical.

The observation of the ESR spectra for triphenyltin radicals generated from single crystals (4), rigid glass solution and in liquid solution (2,5-8) has been of considerable interest in the last several years. Single crystal spectra have revealed a great deal about radical structure in those materials restricted to a crystal matrix. The spectra of randomly oriented samples, such as those formed in rigid glass and liquid solution, have been of low quality. In these systems it has proven difficult to resolve anisotropic spectral features. Therefore, little is understood about the structure of randomly oriented radicals.

Determination of the structure of aryltin radicals also suggests a method to investigate the existence of tin-carbon multiple bonds. IR, NMR and UV studies of multibond character in tetraryl tin and triphenyltin anion have been reported by several investigators (9, 10, 11). These results suggested the need for detailed ESR investigations of aryltin radicals.

Numerous experiments have been reported in the literature for the preparation of aryltin radicals: (a) in situ using UV irradiation of di-t-butyl peroxide with the corresponding hydride dissolved in n-pentane or n-hexane (7); (b) UV photo-chemical bond cleavage of triphenyl-1-cyclopentadienyl tin, (12); (c) x-irradiated single crystal of tetraphenyltin (4); (d) gamma-ray bombardment of glassy beads of finely ground powders at 77 K (3).

In general the methods used to generate triaryltin radicals have involved high energy irradiation (3, 4, 7, 13). However, a key problem in such procedures is simultaneous production of undetermined radical species. These materials complicate the identification of the triaryltin radical and have led to errors in the literature, (5, 13).

Organotin radical structure information generated from ESR data depends on the presence of either of two tin isotopes, ^{119}Sn , and ^{117}Sn . These stable isotopes are necessary to provide critical isotropic and anisotropic hyperfine splitting. Because of their low natural abundance, (8.7% and 7.6%, respectively), it is difficult

to obtain reliable data from isotopically unenriched randomly oriented samples. Line broadening effects caused by random orientation, matrix effects, and unresolved hyperfine splitting make observation of hyperfine interactions nearly impossible.

In this study, triaryltin radicals were generated from isotopically enriched (^{119}Sn 84%) tetraphenyltin, tetrakisparatolytin, and tetrakisorthotolytin. The isotropic and anisotropic hyperfine splittings were determined from ESR spectra. A semi-empirical approach was used to estimate the percent "S" and "P" character of the orbital containing the unpaired electron, the extent of hybridization, the out-of-plane angle, θ , and ligand-tin-ligand inter-bond angle, $\bar{\alpha}$.

II. GENERAL
THEORETICAL CONSIDERATIONS

The general Hamiltonian, \hat{H} used in analysis of ESR spectra is given by:

$$\hat{H} = \hat{H}_Z + \hat{H}_N + \hat{H}_H \quad (1)$$

The first term in equation (1) \hat{H}_Z , refers to the electronic Zeeman effect, the second, \hat{H}_N , to the nuclear Zeeman effect, and the last term, \hat{H}_H , describes the hyperfine coupling.

This Hamiltonian may be written as (14):

$$\hat{H} = \beta \hat{S} \cdot \tilde{g} \cdot \hat{H} - \beta_N \hat{I} \cdot g_N \cdot \hat{H} + \hat{I} \cdot \tilde{A} \cdot \hat{S} \quad (2)$$

\hat{S} and \hat{I} are, respectively, the electronic and nuclear spin vectors, \tilde{g} and g_N are the Lande g-factors for the electron and nucleus, β and β_N are the electronic Bohr magneton and nuclear magneton, and \hat{H} is the applied magnetic field.

II. A \hat{H}_z - ELECTRONIC ZEEMAN EFFECT

Anisotropy in g arises from coupling of the spin angular momentum with the orbital angular momentum. The Hamiltonian is given by:

$$\hat{H} = \beta (\hat{S} \cdot \tilde{g} \cdot \hat{H}) \quad (3)$$

where β is the Bohr magneton. Equation 3 can be written in matrix form as (15):

$$\hat{H} = \beta \begin{bmatrix} S_x & S_y & S_z \end{bmatrix} \begin{bmatrix} g_{xx} & g_{xy} & g_{xy} \\ g_{yx} & g_{yy} & g_{yz} \\ g_{zx} & g_{zy} & g_{zz} \end{bmatrix} \begin{bmatrix} H_x \\ H_y \\ H_z \end{bmatrix} \quad (4)$$

Since S_x , S_y , and S_z as well as H_x , H_y , and H_z are defined in terms of the molecular coordinate x, y, z system, they can be replaced by the same direction cosines. If we define axes X, Y , and Z that diagonalize the g -tensor and pick as an example the case in which they are coincident with the molecular axes, the effective value of g for an arbitrary orientation of the system is then given by:

$$g_{\text{eff}}^2 = g_{xx}^2 \cos^2 \theta_{Hx} + g_{yy}^2 \cos^2 \theta_{Hy} + g_{zz}^2 \cos^2 \theta_{Hz}.$$

$$g_{\text{eff}}^2 = g_{xx}^2 l_x^2 + g_{yy}^2 l_y^2 + g_{zz}^2 l_z^2. \quad (5)$$

Here θ_{Hx} , θ_{Hy} , and θ_{Hz} , are the angles between the applied field H and the X, Y and Z axes, respectively. The symbols l_x , l_y , and l_z are used to represent the cosines of these angles and are referred to as the direction cosines, ($l_x^2 + l_y^2 + l_z^2 = 1$).

Equation (5) can be indicated in matrix notation as:

$$g_{\text{eff}}^2 = [l_x \ l_y \ l_z] \begin{bmatrix} g_{xx}^2 & 0 & 0 \\ 0 & g_{yy}^2 & 0 \\ 0 & 0 & g_{zz}^2 \end{bmatrix} \begin{bmatrix} l_x \\ l_y \\ l_z \end{bmatrix} \quad (6)$$

The molecular coordinate system that diagonalizes the g-tensor may not be coincident with the arbitrary axes associated with the molecule. Equation (6) has to be rewritten in nondiagonal form as:

$$g_{\text{eff}}^2 = [l_x \ l_y \ l_z] \begin{bmatrix} g_{xx}^2 & g_{xy}^2 & g_{xz}^2 \\ g_{yx}^2 & g_{yy}^2 & g_{yz}^2 \\ g_{zx}^2 & g_{zy}^2 & g_{zz}^2 \end{bmatrix} \begin{bmatrix} l_x \\ l_y \\ l_z \end{bmatrix} \quad (7)$$

Consider the first case where the system is mounted with the y-axis perpendicular to the field so that the system can be rotated around y with H making different angles, θ , to z in the xz plane. Now $l_z = \cos \theta$, and $l_x = \sin \theta$, where θ is the angle between H and the z-axis. Substituting these quantities into equation (7) and carrying out the matrix multiplication yields:

$$g_{\text{eff}}^2 = g_{xx}^2 \sin^2 \theta + 2 g_{xz}^2 \sin \theta \cos \theta + g_{zz}^2 \cos^2 \theta \quad (8)$$

For rotations in the yz plane, we have $l_x = 0$, $l_y = \sin \theta$ and $l_z = \cos \theta$. Substitution into equation 7 and matrix multiplication then yield:

$$g_{\text{eff}}^2 = g_{yy}^2 \sin^2 \theta + 2 g_{yz}^2 \sin \theta \cos \theta + g_{zz}^2 \cos^2 \theta \quad (9)$$

In a similar fashion, rotation in the xy plane yields:

$$g_{\text{eff}}^2 = g_{xx}^2 \sin^2 \theta + 2 g_{xy}^2 \sin \theta \cos \theta + g_{yy}^2 \cos^2 \theta \quad (10)$$

For species of threefold or higher symmetry where the molecular coordinate system diagonalizes the g-tensor, $x=y$. Therefore, the general Hamiltonian may be rewritten as (16):

$$\begin{aligned} \hat{H} = & \beta g_{\parallel} \hat{H}_z \hat{S}_z + \beta g_{\perp} (\hat{H}_x \hat{S}_x + \hat{H}_y \hat{S}_y) + A_{\parallel} \hat{S}_z \hat{I}_z \\ & + A_{\perp} (\hat{S}_x \hat{I}_x + \hat{S}_y \hat{I}_y) - g_N \beta_N \hat{H} \hat{I} \end{aligned}$$

The g-value for any orientation is given by:

$$g^2 = g_{\perp}^2 \sin^2 \theta + g_{\parallel}^2 \cos^2 \theta$$

where θ is the angle that the g axis makes with the applied field. g_{\perp} and g_{\parallel} are the g-factor values for a magnetic field oriented perpendicular and parallel to the symmetry axis.

Since many more molecules have g_{\perp} aligned than g_{\parallel} the most intense absorption will correspond to g_{\perp} as shown in figure 1, (15). The absorption spectrum (which includes the effects of the probabilities of the various orientations and the transition probability corresponding to each of these), is shown in figure 2, (14).

In the case where a molecule is rapidly tumbling, it is possible to observe an isotropic value of g. Radicals in liquid solutions are good examples of this. The isotropic g-factor, g_{iso} , can be determined from g_{\perp} and g_{\parallel} as follows:

$$g_{iso} = 1/3 (g_{\parallel} + 2g_{\perp})$$

Figure 1 - The distribution of g_{\perp} and g_{\parallel} in a randomly oriented sample with a threefold or higher symmetry axis.

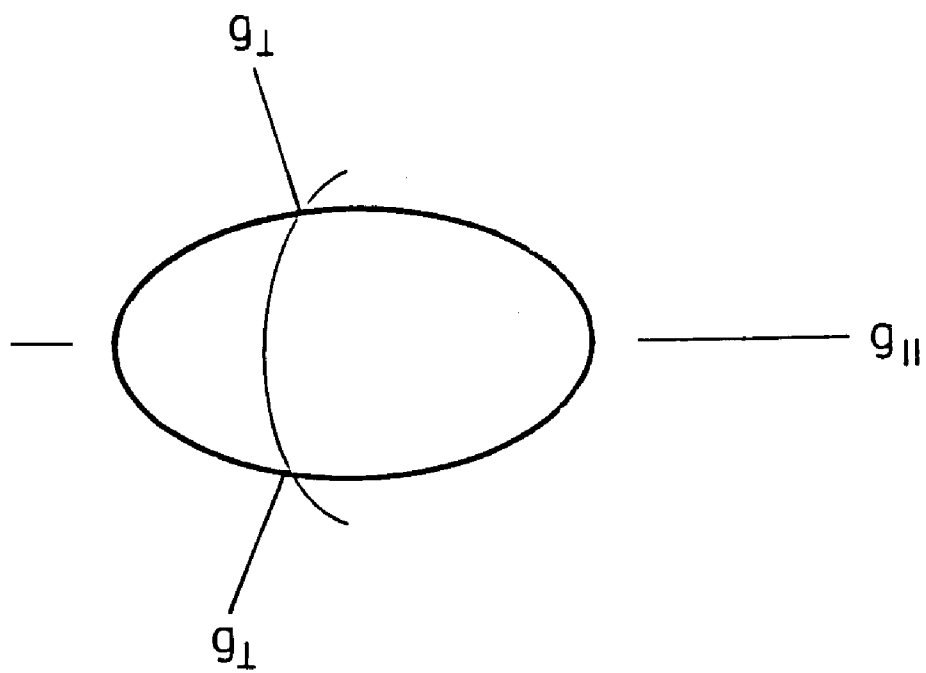


Figure 2 - Absorption line shape for axial symmetry with g-factor anisotropy.

A. Integral

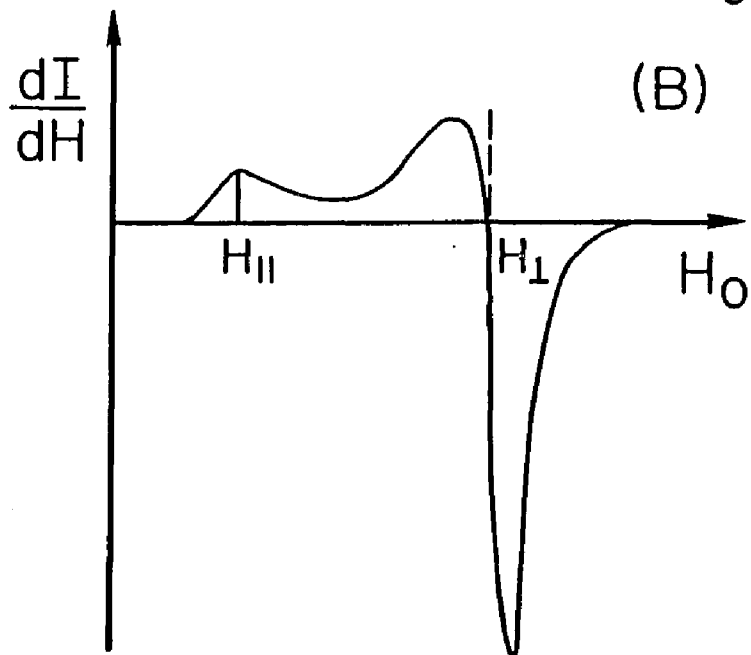
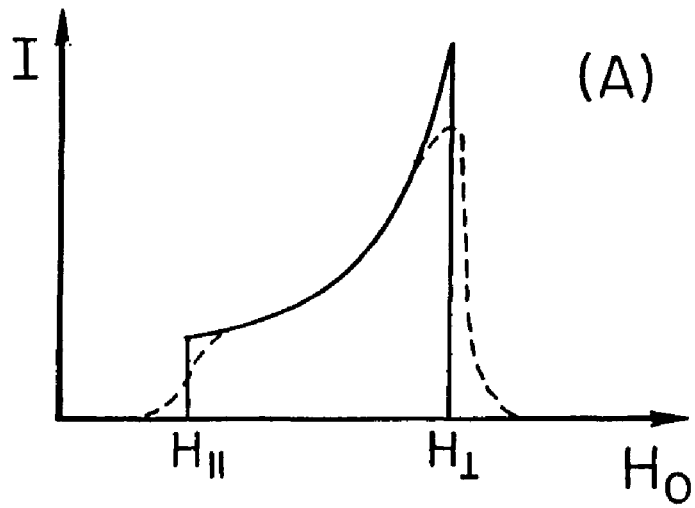
B. Differential

I = intensity

H_0 = applied magnetic field

H_{\perp} = magnetic field at g_{\perp}

H_{\parallel} = magnetic field at g_{\parallel}



II . B \hat{M}_H - HYPERFINE COUPLING

The interaction of an unpaired electron and a magnetic nucleus is called the nuclear hyperfine interaction. The hyperfine interaction may be either anisotropic (orientation-dependent) or isotropic (independent of the orientation of H with respect to a molecular axis).

ESR spectra of triaryltin radicals in an inert matrix show that the hyperfine coupling interaction contains both isotropic hyperfine (a) and anisotropic hyperfine splitting (τ) components (14).

1 - Anisotropic Hyperfine Coupling

In rigid systems, the electron and nuclear dipole coupling give rise to anisotropy in the electron nuclear hyperfine components. The classical expression for the dipolar coupling of a fixed electron and nucleus separated by a distance r is (15):

$$W_{\text{dipolar}} = \frac{\hat{U}_e \cdot \hat{U}_N}{r^3} - \frac{3(\hat{U}_e \cdot \hat{r})(\hat{U}_N \cdot \hat{r})}{r^5} \quad (11)$$

Here \hat{r} represents the vector joining an electron and a nucleus. \hat{U}_e and \hat{U}_N are, respectively, the electron and nuclear magnetic moments. For a quantum mechanical system, the magnetic moments must be replaced by their corresponding operator. The Hamiltonian is:

$$\hat{H}_{\text{dipolar}} = -g \beta g_N \beta_N \left[\frac{\hat{S} \cdot \hat{I}}{r^3} - \frac{3(\hat{S} \cdot \hat{r})(\hat{I} \cdot \hat{r})}{r^5} \right] \quad (12)$$

Substituting $\hat{S} = \hat{S}_x + \hat{S}_y + \hat{S}_z$, $\hat{I} = \hat{I}_x + \hat{I}_y + \hat{I}_z$, and

$\hat{r} = x\hat{i} + y\hat{j} + z\hat{k}$ leads to:

$$\begin{aligned} \hat{H}_{\text{dipolar}} = & -g \beta g_N \beta_N \left[\left[\frac{r^2 - 3x^2}{r^5} \right] \hat{S}_x \hat{I}_x + \left[\frac{r^2 - 3y^2}{r^5} \right] \hat{S}_y \hat{I}_y + \right. \\ & \left[\frac{r^2 - 3z^2}{r^5} \right] \hat{S}_z \hat{I}_z - \left[\frac{3xy}{r^3} \right] (\hat{S}_x \hat{I}_y + \hat{S}_y \hat{I}_x) - \\ & \left. \left[\frac{3xz}{r^3} \right] (\hat{S}_x \hat{I}_z + \hat{S}_z \hat{I}_x) - \left[\frac{3yz}{r^3} \right] (\hat{S}_y \hat{I}_z + \hat{S}_z \hat{I}_y) \right] \quad (13) \end{aligned}$$

When this Hamiltonian is applied to an electron in an orbital, the quantities in brackets must be replaced by average values over the electronic wave function.

$$\hat{H}_{\text{dipolar}} = - (g_B g_N \beta_N) [\hat{S}_x \hat{S}_y \hat{S}_z] \begin{bmatrix} \langle \frac{r^2 - 3x^2}{r^5} \rangle & \langle \frac{-3xy}{r^5} \rangle & \langle \frac{-3xz}{r^5} \rangle \\ \langle \frac{-3xy}{r^5} \rangle & \langle \frac{r^2 - 3y^2}{r^5} \rangle & \langle \frac{-3yz}{r^5} \rangle \\ \langle \frac{-3xz}{r^5} \rangle & \langle \frac{-3yz}{r^5} \rangle & \langle \frac{r^2 - 3z^2}{r^5} \rangle \end{bmatrix} \begin{bmatrix} \hat{I}_x \\ \hat{I}_y \\ \hat{I}_z \end{bmatrix} \quad (14)$$

This equation is abbreviated as:

$$\hat{H}_{\text{dipolar}} = h \hat{S} \cdot \tilde{T} \cdot \hat{I} \quad (15)$$

where \tilde{T} is the dipolar interaction tensor, and h is Planck's constant. It assumes the same general form as the g -tensor in equation 7. For example, $\langle r^2 - 3x^2 / r^5 \rangle = T_{xx}$ and $\langle -3xy / r^5 \rangle = T_{xy}$.

The dipolar interaction tensor can be diagonalized to yield a measure of the anisotropic hyperfine interaction. For example, consider the electron to be in a P_z orbital. By converting to spherical polar coordinates and by substituting $z=r \cos\theta$, $x=r \sin\theta \cos\bar{\phi}$ and $y=r \sin\theta \sin\bar{\phi}$, the result for an electron at a specific (r, θ) is:

$$T_{zz} = g \beta g_N \beta_N \langle (3 \cos^2 \theta - 1) / r^3 \rangle \quad (16)$$

$$T_{yy} = -\frac{1}{2} g \beta g_N \beta_N \langle (3 \cos^2 \theta - 1) / r^3 \rangle \quad (17)$$

$$T_{xx} = -\frac{1}{2} g \beta g_N \beta_N \langle (3 \cos^2 \theta - 1) / r^3 \rangle \quad (18)$$

Now consider that the electron can be located at any place in the p-orbital. Thus, we have to integrate over all possible angles for the radius vector to the electron in this orbital and then over all radii r . The result is

$$T_{zz} = \frac{4}{5} g \beta g_N \beta_N \langle \frac{1}{r^3} \rangle = 2B_0 \quad (19)$$

$$T_{xx} = -\frac{2}{5} g \beta g_N \beta_N \langle \frac{1}{r^3} \rangle = -B_0 \quad (20)$$

$$T_{yy} = -\frac{2}{5} g \beta g_N \beta_N \langle \frac{1}{r^3} \rangle = -B_0 \quad (21)$$

where $\langle \frac{1}{r^3} \rangle$ is the average value of the quantity $\frac{1}{r^3}$.

2 - Isotropic Hyperfine Coupling

The isotropic hyperfine coupling is given by:

$$H = a \hat{S} \cdot \hat{I} \quad (22)$$

The $a \hat{S} \cdot \hat{I}$ term describes the coupling of the electron and nuclear spin moments, which classically corresponds to the dot product of these two vectors. The quantity a indicates the magnitude of the interaction and has the dimensions of energy. This is referred to as the Fermi contact contribution to the coupling, and its magnitude depends upon the amount of electron density at the nucleus $|\psi(0)|^2$ according to

$$A_0 = \frac{8\pi}{3} g \beta g_N \beta_N |\psi(0)|^2 \quad (23)$$

$|\psi(0)|^2$ is only non-zero if the unpaired electron is in an S-orbital (14). Spectral analysis requires the comparison of the calculated value A_0 , with the experimentally determined $a = a_{iso}$.

3 - The Breit-Rabi Equation

All atoms with one electron, $I = \frac{1}{2}$, give an anomalous Zeeman effect in a weak magnetic field. This is due to the effect of the spin magnetic moment of the electrons on the splitting of the levels in the ground state and in the excited state. A weak magnetic field is one in which the interaction between the magnetic moment of the atom and the applied field is of the same magnitude as the hyperfine coupling, A .

When the hyperfine components are very small compared to the applied field the transition occurs at: $h\nu = \pm \frac{1}{2}A + g\beta H$. The spectrum is therefore, a doublet symmetrically disposed about the resonance position for a radical with zero nuclear spin (H_0). For a hyperfine interaction of the same order of magnitude as the applied field, the quantization axis is no longer fully determined by the applied field. The variation of the energy levels is, therefore, non-linear in the applied field. The doublet is then unsymmetrically disposed about H_0 . The Hamiltonian now becomes:

$$\hat{H} = \beta \hat{S} \cdot \tilde{g} \cdot \hat{H} - g_N \beta_N \hat{H} \cdot \hat{I} + h \hat{S} \cdot \tilde{A} \cdot \hat{I} \quad (24)$$

where the first term is the electronic Zeeman term, the second is the nuclear Zeeman term, and the third is the hyperfine interaction term. The quantity A in the third term includes both the isotropic and anisotropic components of the hyperfine interaction:

$$A = T + a \quad (25)$$

A is not to be confused with A_0 , the calculated value for the isotropic hyperfine splitting. The magnitude of the hyperfine interaction (for the case where it is comparable to the applied magnetic field) where $I = \frac{1}{2}$, and where the system has axial symmetry, can be expressed by the Breit-Rabi equation (17, 18). Indicated below is a suitable solution (19, 20):

$$W = \frac{-\Delta W}{2(2I+1)} + g_n \beta_n H M_F \pm \frac{\Delta W}{2} \left[\frac{1 + 4M_F x + x^2}{(2I+1)} \right]^{\frac{1}{2}} \quad (26)$$

where $\Delta W = (2I+1)A/2$, $x = (g - g_n)\beta H / \Delta W$, $F = I \pm S$ and $M_F = \pm F$.

W is the energy separation of hyperfine levels, and $M_F =$ levels of z component of combined electron and nuclear moment. A simple solution is for the case where $I = \frac{1}{2}$ and direct nuclear interactions can be neglected. The equation then becomes (17, 20)

$$A_{||} = \frac{2H_0(H_0 - H_k)}{2H_0 - H_k} \quad (27)$$

$$A_{\perp} = \frac{2H_0(H_1 - H_0)}{2H_0 - H_1} \quad (28)$$

A is the hyperfine splitting, and H_0 , H_k , and H_1 are the field positions of central line, low-field satellite, and high-field satellite. The overall result is that when the hyperfine splitting is not very small compared to the applied field, the true hyperfine splitting is less than the distance measured between absorption lines and the g-value is less than that measured at the center signal of the spectrum.

A computer program shown in Appendix A, which uses the position of the satellite line and the observed field position of the central line was written to calculate coupling constants, S-character, P-character, hybridization, ligand-tin-ligand bond angles and out-of-plane bond angles for aryltin radicals of C_{3v} symmetry.

II. C \hat{H}_N - NUCLEAR ZEEMAN INTERACTION

The nuclear Zeeman Hamiltonian represents the interaction of the proton spin with the external magnetic field (15). The nuclear interaction with the field will be isotropic and represented as a scalar.

The net effect of the nuclear Zeeman interaction is to simultaneously raise the positions of the electronic energy levels leaving the difference in the energy levels unchanged. The observed spectra will then be essentially unaffected by this contribution (21).

II. D SPECTRAL ANALYSIS

The principal aim of the analysis of ESR spectra is to obtain the experimental parameters which would make it possible, after comparison with atomic constants, to estimate the "S" character, C_s^2 , and "P" character, C_p^2 of the atomic orbital containing the unpaired electron (14). Hartree-Fock calculations have made available the theoretical values of $|\psi(0)|^2$ and $\langle \frac{1}{r^3} \rangle$ for each element of the Periodic Table (22, 23-25). Thus, it is possible using equation 23, and 19-21, respectively, to calculate the isotropic coupling constant, A_0 , and the anisotropic coupling constants, $2B_0$, $-B_0$, $-B_0$, associated, respectively, with the ns and np orbitals of each atom.

$$C_s^2 = \frac{a_{iso}}{A_0} \quad (29)$$

where a_{iso} and A_0 are, respectively, experimental and calculated hyperfine splitting values.

$$C_p^2 = \frac{\tau_z}{2B_0} \quad (30)$$

Where τ_z and $2B_0$ are, respectively, experimental and calculated anisotropic hyperfine splitting values.

When the values of C_s^2 , and C_p^2 are determined, one can calculate the hybridization ratio, λ^2 , and use it to estimate structural parameters:

$$\lambda^2 = \frac{C_p^2}{C_s^2} \quad (31)$$

$$\bar{\epsilon} = \cos^{-1} \left[\frac{1.5}{2 \lambda^2 + 3} - \frac{1}{2} \right] \quad (32)$$

$$\cos^2 \theta = \frac{1}{3} [1 + 2 \cos \bar{\epsilon}] \quad (33)$$

where $\bar{\epsilon}$ is the interbond angle (ligand-metal-ligand) and θ is the complement of the ligand-tin-symmetry axis angle.

Correct values can only be obtained by application of the Breit-Rabi equation (17-20)

$$A_{\parallel} = \frac{2H_0(H_0 - H_K)}{2H_0 - H_K} \quad (34)$$

$$A_{\perp} = \frac{2H_0(H_1 - H_0)}{2H_0 - H_1} \quad (35)$$

A is the hyperfine splitting, and H_0 , H_K , and H_1 are the field positions of central line, low-field satellite, and high-field satellite.

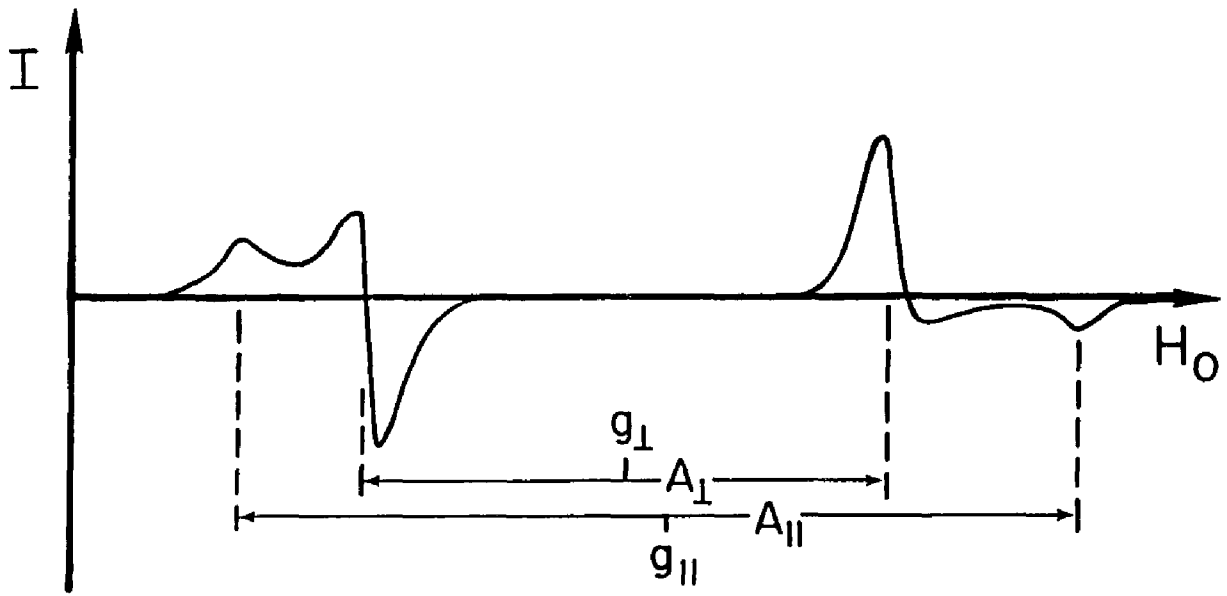
When the values of $A_{||}$ and A_{\perp} are determined, the isotropic and anisotropic hyperfine splitting can be calculated using the following equations:

$$a_{iso} = 1/3 (A_{||} + 2A_{\perp}) \quad (36)$$

$$\tau_{\perp} = 1/3 (A_{||} - A_{\perp}) \quad (37)$$

From the analyses of ESR spectra of triaryltin radicals, the satellites corresponding to $A_{||}$ will be furthest upfield and furthest downfield, that is fall on the outside of the spectra. Those corresponding to A_{\perp} , will be between the $A_{||}$ spectral features, that is on the inside of the spectra as shown in figure 3 (1).

Figure 3 - Powder ESR spectrum for a hypothetical radical with $S = \frac{1}{2}$, $I = \frac{1}{2}$ axial symmetry, $g_{\parallel} > g_{\perp}$ and $A_{\parallel} > A_{\perp}$.

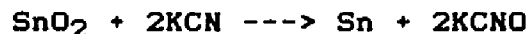


III. Experimental

A - Synthesis

PREPARATION OF METALLIC TIN

Tin has been prepared according to the method of Biltz (26) by the reduction of stannic oxide.



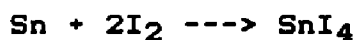
Starting Materials: Stannic oxide, potassium cyanide and sodium hydroxide were used as supplied from Fisher.

Apparatus: Porcelain crucible and Meker burner.

Procedure: Heat a mixture of 1.0 gram of finely powdered stannic oxide and 1.3 grams of potassium cyanide in a porcelain crucible for twenty minutes over a Meker burner. After cooling, wash the regulus of metallic tin with a dilute solution of sodium hydroxide, then with water to give 0.712g (90%) yield (lit. 76-95%).

PREPARATION OF STANNIC IODIDE

Stannic iodide has been prepared by the reaction of iodine and tin in carbontetrachloride as a solvent (27).



An excess of tin prevents contamination of the product with iodine.

Starting materials: Tin was prepared as previously described. Iodine and carbontetrachloride were used as supplied from Fisher.

Apparatus: Buchner funnel, 250-mL round-bottom flask provided with a reflux condenser fitted with a calcium chloride tube, heating mantle.

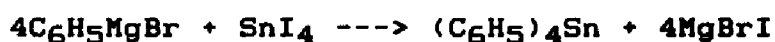
Procedure: 1.2 grams of tin (0.0101 mole) and 4.0 grams of iodine (0.0157 mole) were placed in a 100-mL round-bottom flask. Twenty five milliliters of carbontetrachloride were added and a reflux condenser was attached. The flask was heated until the reaction began.

When the solution stopped boiling, it was heated until all iodine had sublimed as was evidenced by a change in color of the liquid from violet to orange-yellow, and by the absence of colored vapors in the flask and reflux condenser.

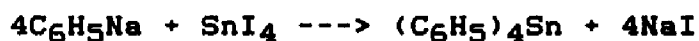
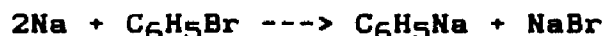
The hot solution was filtered quickly using Buchner filtration. The filtrate was cooled to give 5.6g (90%) yield of a red crystalline stannic iodide which melted at 142-143.5°C (lit. 143.5°C).

PREPARATION OF TETRAPHENYLTIN

Three procedures have been used to prepare tetraphenyltin compounds (28-30).

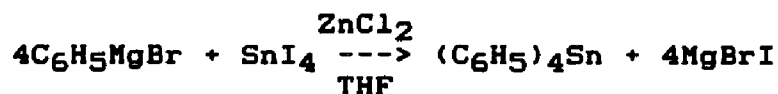


or



These preparations involved the action of an organometallic compound (Grignard) on stannic iodide and the reaction of arylhalides and stannic iodide with sodium in refluxing ether or benzene. The former method is superior. In general the yield of organotin compound is between 40% and 70%. An excess of the Grignard reagent was usually required for a higher yield. Even so, the product may have contained some of the triaryltin iodide.

A yield above 90% of tetraphenyltin was obtained by using organozinc reagents (30).



Starting Materials: Magnesium and bromobenzene were used as supplied from Aldrich. Stannic iodide was prepared as previously described. Benzene and tetrahydrofuran were distilled from calcium hydride and stored over sodium wire. Nitrogen gas was dried by passing through concentrated sulfuric acid.

Apparatus: 250-mL 3-necked boiling flask, provided with a reflux condenser fitted with a calcium chloride tube, a dropping funnel and tube through which gaseous nitrogen could be introduced.

Procedure: The flask was dried thoroughly with a flameless heat gun while flushing with dry nitrogen. A solution of 15.7 grams (0.1 mole) of bromobenzene in 20.0 milliliters of dry tetrahydrofuran was added dropwise to a solution of 2.5 grams (0.103 mole) of magnesium in 15.0 milliliters of dry tetrahydrofuran. The flask was heated gently until the reaction began, after which heating was no longer necessary. After the addition, the reaction mixture was refluxed for one hour. A solution of 6.26 grams (0.01 mole) of stannic iodide in 50.0 milliliters of dry benzene was added dropwise to the reaction mixture. After the addition, the reaction mixture was refluxed for two hours and then carefully hydrolyzed with 10% hydrochloric acid. The organic layer was separated, washed

with water, and dried over anhydrous sodium sulfate. The organic layer was concentrated and cooled to yield 65% of raw product. After a recrystallization from benzene, 55% of pure product (white needles of tetraphenyltin) was obtained melting at 226-227°C (lit. 226-228°C and 229°C). $^1\text{H-NMR}$ and IR are consistent with known literature values (31). Schwarzkopf analysis for tetraphenyltin, found 66.99% C and 4.81% H. The theoretical values are 67% C and 5% H.

Zinc Catalyst Modification

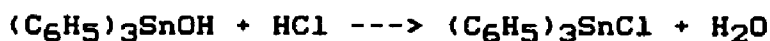
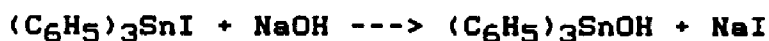
A yield above 90% of tetraphenyltin was obtained by using organozinc reagents. After phenylmagnesium bromide was prepared, a suspension of dry zinc chloride in dry tetrahydrofuran was added through the dropping funnel. Reaction took place immediately. Then, stannic iodide in dry benzene was added dropwise. After addition, the reaction was refluxed for two hours and then hydrolyzed with 10% hydrochloric acid. The organic layer was separated, washed with water and dried over sodium sulfate. The organic layer was concentrated and cooled to yield 90% of tetraphenyltin, melting at 226-228°C (lit. 224-225°C). $^1\text{H-NMR}$ and IR are consistent with literature values (31, 9).

PREPARATION OF TRIPHENYLTIN CHLORIDE

Two procedures have been used to prepare triphenyltin chloride according to the methods of Kozeschkow (32) and Chambers (30).



or



These preparations involved heating tetraphenyltin with stannic chloride in an oil bath at 220-240°C for 3 hours, or employing the method of Chambers. The latter method is superior.

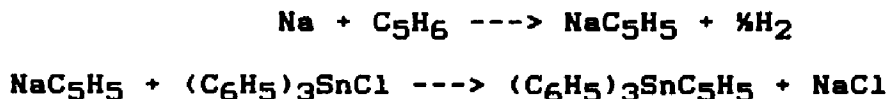
Starting Materials: Iodine and chloroform were used as supplied from Fisher. Tetraphenyltin was prepared as previously described.

Apparatus: 250-mL round-bottom flask, provided with a reflux condenser fitted with a calcium chloride tube and a heating mantle.

Procedure: In small lots, 0.9 grams (3.54×10^{-3} mole) of iodine were added to 1.5 grams (3.5×10^{-3} mole) of tetraphenyltin in 25.0 milliliters of chloroform. After each addition of iodine the solution immediately became decolorized. Iodine was added until a permanent brown color was obtained which was not discharged after boiling for one hour. The solvent was removed on the water-bath and iodobenzene was removed by distilling under reduced pressure. The residue was dissolved in ether and filtered to remove unreacted tetraphenyltin. The ether solution was shaken with 30% sodium hydroxide solution, and the layers were separated. The ether layer was shaken with concentrated hydrochloric acid, the layers were separated and the ether was dried over sodium sulfate. On concentration of the ether solution, 0.7 grams (52%) of triphenyltin chloride were obtained which after recrystallization from ether melted at $105-106^{\circ}\text{C}$, (lit. 106°C). $^1\text{H-NMR}$ and IR are consistent with known literature values (31, 9).

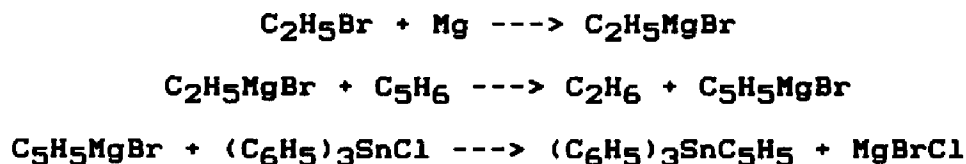
PREPARATION OF TRIPHENYL-1-CYCLOPENTADIENYL TIN (TPC)

Several routes are possible for the preparation of triphenyl-1-cyclopentadienyltin, (TPC). Among them is the use of alkali metals to form the corresponding salts which then could react further with triphenyltin chloride (29).



However, some of these salts are spontaneously flammable on exposure to air.

The Grignard method offered a convenient and safe way to arrive at this compound (33, 34).



Cyclopentadienylmagnesium bromide was prepared according to the method of Grignard and Courtot (33) using an exchange reaction between cyclopentadiene and ethylmagnesium bromide. This Grignard compound then was treated with

triphenyltin chloride (34). Freshly prepared cyclopentadienyl was used and a benzene-ether, (1:1) mixture, was employed as a solvent. Cyclopentadienyl derivatives of tin are unstable in the presence of air and light.

Starting Materials: Triphenyltin chloride was prepared as previously described. Cyclopentadiene was obtained by cracking dicyclopentadiene with a short distilling column, packed with glass wool. Cyclopentadiene was distilled twice and stored in an ice bath until ready for use. Benzene and petroleum ether were distilled from calcium hydride and stored over sodium wire. Diethyl ether was dried by storing over sodium wire. All operations involving the use of Grignard reagents were run in a nitrogen atmosphere.

Apparatus: 250-mL 3-necked boiling flask, provided with a reflux condenser fitted with a calcium chloride tube, a dropping funnel and tube through which gaseous nitrogen could be introduced.

Procedure: The flask was thoroughly dried with a flameless heat gun while flushing with dry nitrogen. Cyclopentadienylmagnesium bromide was prepared according to the method of Grignard and Courtot (33). A solution of 0.8

milliliters (0.01 mole) of freshly distilled cyclopentadiene in 40.0 milliliters of dry benzene was added slowly to an ethyl-magnesium bromide solution, prepared from 0.24 grams (0.01 mole) of magnesium in 10.0 milliliters of dry ether and 0.8 milliliters (0.01 mole) of ethyl bromide in 10.0 milliliters of dry ether, followed by heating for 1.5 hours at 60°C with the evolution of ethane. Cyclopentadienylmagnesium bromide formed a dark colored clear solution. A solution of 1.5 grams (3.9×10^{-3} mole) of triphenyltin chloride in 32.0 milliliters of a benzene-ether (1:1) mixture, was added rapidly to the solution of cyclopentadienylmagnesium bromide. After heating the reaction mixture for four hours at the reflux temperature, it was concentrated to a yellow, oily paste by distillation of the mixed solvents at reduced pressure. This paste was digested twice with 100.0 milliliters of a benzene-petroleum ether, (1:1) mixture, (b.p. 60-80°C) and filtered hot. After concentrating and cooling the filtrate, 1.2 grams (80%) of triphenyl-1-cyclopentadienyltin were obtained. After two recrystallizations from petroleum ether (b.p. 60-80°C) one gram of pure product, (light yellow crystals) was obtained melting at 122-124°C (lit. 130-131°C, 129°C and 120°C).

^1H -NMR, and pseudo rotation of TPC are reported. The five cyclopentadienyl protons showed only one sharp signal at 377Hz (lit. 368.5Hz), which has satellites at both sides originating from H- ^{119}Sn and H- ^{117}Sn coupling (35). These results appear to be consistent with literature values (35).

PREPARATION OF TRIPHENYLTIN HYDRIDE

Triphenyltin hydride has been prepared according to the method of Kuivila (36).



Starting Materials: Triphenyltin chloride was prepared as previously described. Lithium aluminum hydride was used as supplied from Aldrich. Diethyl ether was dried by storing over sodium wire.

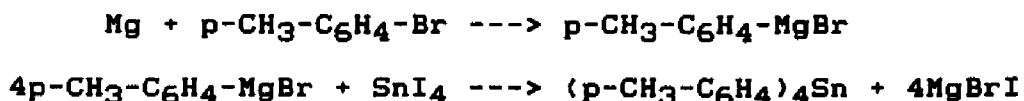
Apparatus: 250-ml 3-necked boiling flask, provided with a reflux condenser fitted with a calcium chloride tube, a dropping funnel and tube through which gaseous nitrogen could be introduced.

Procedure: The flask was dried thoroughly with a flameless heat gun while flushing with dry nitrogen. 13.0 grams of triphenyltin chloride and 0.8 grams of lithium aluminum hydride were added rapidly to 150 milliliters of dry ether, which was cooled in an ice-bath. The mixture was stirred at the bath temperature for 15 minutes, and then at room temperature for three hours. The ice-water was carefully added until there was no further evidence

of gas evolution. The ether layer was separated, washed several times with water and dried over anhydrous magnesium sulfate. The ether solution was then distilled at reduced pressure to give a gray viscous oil. The oil was vacuum distilled to yield a white liquid, boiling point 155-162°C (lit. 162-168 at .5mm). On exposing this white liquid to air, it became a gray viscous material. ¹H-NMR and IR are consistent with known literature values (37, 38).

PREPARATION OF TETRAKISPARATOLYL TIN

Tetrakis(p-tolyl)tin has been prepared according to the method of Krause (39).



After two recrystallizations from a benzene-chloroform, (1:1) mixture, a 43% yield of pure product was obtained melting at 233-235°C (lit. 233-237°C).

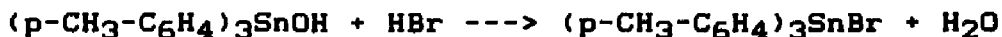
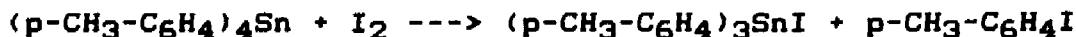
Starting Materials: Magnesium and 4-bromotoluene were used as supplied from Aldrich. Stannic iodide was prepared as previously described. Benzene and tetrahydrofuran were distilled from calcium hydride and stored over sodium wire. Nitrogen gas was dried by passing through concentrated sulfuric acid.

Apparatus: 250-ml 3-necked boiling flask, provided with a reflux condenser fitted with a calcium chloride tube, a dropping funnel and tube through which gaseous nitrogen could be introduced.

Procedure: The flask was dried thoroughly with a flameless heat gun while flushing with dry nitrogen. A solution of 5.173 grams (.030 mole) of 4-bromotoluene in 20.0 milliliters of dry tetrahydrofuran was added dropwise to a solution of 0.81 grams (.0333 mole) of magnesium in 15.0 milliliters of dry tetrahydrofuran. The flask was heated gently until the reaction began, after which heating was no longer necessary. After the addition, the reaction mixture was refluxed for one hour. A solution of 3.3 grams (5.3×10^{-3} mole) of stannic iodide in 50.0 milliliters of dry benzene was added dropwise at room temperature to the reaction mixture. After the addition, the reaction was refluxed for 18 hours and then carefully hydrolyzed with 10% hydrochloric acid. The organic layer was separated, washed with water, and dried over anhydrous sodium sulfate. The organic layer which was concentrated and cooled yielded 50% of raw product. After two recrystallizations from a benzene-chloroform, (1:1) mixture, 1.1 grams (45%) of white, crystalline tetrakis(p-tolyl)tin was obtained melting at 233-235°C (lit. 233-237°C) (39). ¹H-NMR is consistent with known literature values (31). Schwarzkopf analysis for tetrakisparatolytin, found 68.96% C and 5.82% H. The theoretical values are 69% C and 6% H.

PREPARATION OF TRISPARATOLYL TIN BROMIDE

Tris(p-tolyl)tin bromide has been prepared according to the method of Chambers and Scherer (30).



Starting Materials: Iodine, sodium hydroxide, hydrobromic acid and chloroform were used as supplied from Fisher. Tetrakis(p-tolyl)tin was prepared as previously described.

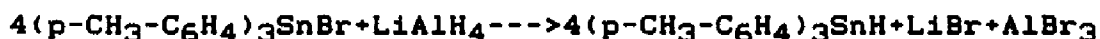
Apparatus: 250-mL round-bottom flask, provided with a reflux condenser fitted with a calcium chloride tube and heating mantle.

Procedure: In small lots, 0.64 grams (2.5×10^{-3} mole) of iodine were added to 1.2 grams (2.5×10^{-3} mole) of tetrakis(p-tolyl)tin in 25.0 milliliters of chloroform. After each addition of iodine the solution immediately became decolorized. Iodine was added until a permanent brown color was obtained which was not discharged after boiling for one hour. The solvent was removed on the

water-bath and iodotoluene was removed by distilling under reduced pressure. The residue was dissolved in ether and filtered to remove unreacted tetrakis(p-tolyl)tin. The ether solution was shaken with 30% sodium hydroxide solution and the layers were separated. The ether layer was shaken with concentrated hydrobromic acid, the layers were separated and the ether layer was dried over anhydrous sodium sulfate. On concentration of the ether solution, 0.7 grams (60%) of tris(p-tolyl)tin bromide were obtained, which after recrystallization from ether melted at 97.5-98.5°C (lit. 98.5°C). ¹H-NMR is consistent with known literature values (31).

PREPARATION OF TRISPARATOLYL TIN HYDRIDE (PTH)

Tris(p-tolyl)tin hydride (PTH) has been prepared according to the method of Becker (40).



Starting Materials: Tris(p-tolyl)tin bromide was prepared as previously described. Lithium aluminum hydride and sodium potassium tartrate were used as supplied from Aldrich and Fisher, respectively. Diethyl ether was dried by storing over sodium wire.

Apparatus: 250-mL 3-necked boiling flask, provided with a reflux condenser fitted with a calcium chloride tube, a dropping funnel and tube through which gaseous nitrogen could be introduced.

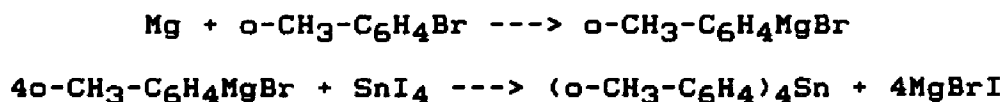
Procedure: The flask was dried thoroughly with a flameless heat gun while flushing with dry nitrogen. A solution of 2.0 grams of tris(p-tolyl)tinbromide dissolved in 25.0 milliliters of dry ether was added dropwise to 0.2 grams of lithium aluminum hydride suspended in 25.0 milliliters of dry ether. After the addition, the reaction mixture was refluxed for two hours and stirred at room

temperature for an additional hour. 10.0 milliliters of water were carefully added until there was no evidence of gas evolution. The contents of the flask were poured into a solution of sodium potassium tartrate. The ether layer was separated, washed several times with water and dried over anhydrous sodium sulfate. The ether solution was then distilled at reduced pressure leaving a white solid melting at 79.5-81°C. Recrystallization from methanol yielded 1.5 grams (75%) of white needles (lit. 88%) melting at 82-84°C (lit. 82.3-84.9°C), (40).

¹H-NMR was consistent with the literature including a sharp signal (Sn-H) at 400Hz (lit. 425Hz). IR showed a sharp signal (Sn-H stretching) at 1240cm⁻¹ (lit. 1240cm⁻¹), (37, 38).

PREPARATION OF TETRAKISORTHOTOLYL TIN

Tetrakis(o-tolyl)tin has been prepared according to the method of Grignard (30).



After three recrystallizations from a benzene-ethanol, (1:1) solvent mixture, a mixture of tetrakis(o-tolyl)tin and hexakis(o-tolyl)ditin were obtained and easily separated. The melting points were 215-217°C and 299°C, respectively (lit. 217.5-219.5°C and 299°C), (35, 8).

Starting Materials: Magnesium and 2-bromotoluene were used as supplied from Aldrich. Stannic iodide was prepared as previously described. Benzene and tetrahydrofuran were distilled from calcium hydride and stored over sodium wire. Nitrogen gas was dried by passing through concentrated sulfuric acid.

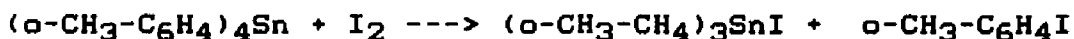
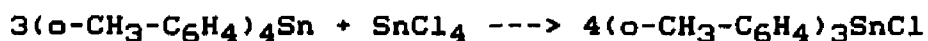
Apparatus: 250-mL 3-necked boiling flask, provided with a reflux condenser fitted with a calcium chloride tube, a dropping funnel and tube through which gaseous nitrogen could be introduced.

Procedure: The flask was dried thoroughly with a flameless heat gun while flushing with dry nitrogen. A solution of 12.0 milliliters (0.1 mole) of 2-bromotoluene in 20.0 milliliters of dry tetrahydrofuran was added dropwise to a solution of 2.43 grams (0.1 mole) of magnesium in 40.0 milliliters of dry tetrahydrofuran. The flask was heated gently until the reaction began, after which heating was no longer necessary. After the addition, the reaction mixture was stirred for one hour at room temperature. A solution of 10.0 grams (0.016 mole) of stannic iodide in 100.0 milliliters of dry benzene was added dropwise at room temperature to the reaction mixture. After the addition, the reaction was refluxed for seven hours and then allowed to stir at room temperature over night. The reaction mixture was then carefully hydrolyzed with 10% hydrobromic acid. The organic layer was separated, washed several times with water, and dried over anhydrous sodium sulfate. The organic layer was concentrated and cooled to form a white precipitate melting at 290°C which was recrystallized from benzene to give 2.4 grams (20%) of hexakis(o-tolyl)ditin melting at 299°C (lit. 299°C) (8). The filtrate was reconcentrated and cooled to yield a white solid. Further recrystallization

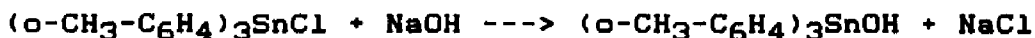
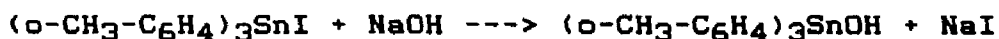
from a benzene-ethanol, (1:1) mixture, gave 1.2 grams (15%) of a white crystalline solid melting at 215-217°C (lit. 217.5-219.5°C) (41). ¹H-NMR is consistent with known literature values (31, 8). Schwarzkopf analysis for tetrakisorthotolytin, found 68.92% C and 5.82% H. The theoretical values are 69% C and 6% H.

PREPARATION OF TRISORTHOTOLYLTIN BROMIDE

Two procedures have been used to prepare tris-(o-tolyl)tin bromide (30, 39). The preparations involve the heating of tetrakis(o-tolyl)tin with stannic chloride in an oil bath, or employing the reaction of tetrakis(o-tolyl)tin or hexakis(o-tolyl)tin and iodine in refluxing chloroform. The latter method is superior producing 60-70% of pure product melting at 98-99.5°C (lit. 99.5°C) (41).



or



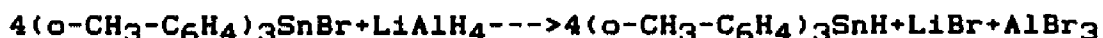
Starting Materials: Iodine, hydrobromic acid, chloroform and potassium hydroxide were used as supplied from Fisher. Hexakis(o-tolyl)ditin and tetrakis(o-tolyl)-tin were prepared as previously described.

Apparatus: 250-mL round-bottom flask, provided with a reflux condenser fitted with a calcium chloride tube and heating mantle.

Procedure: In small lots, 1.25 grams (5.0×10^{-3} mole) of iodine were added to 2.4 grams (3.0×10^{-3} mole) of hexakis(o-tolyl)ditin in 25.0 milliliters of chloroform. After each addition of iodine the solution immediately became decolorized. Iodine was added until a permanent brown color was obtained which was not discharged after boiling for one hour. The solvent was removed on the water-bath. The residue was dissolved in ether and filtered to remove unreacted hexakis(o-tolyl)ditin. The ether solution was shaken with 30% potassium hydroxide solution and the layers were separated. The ether layer was shaken with concentrated hydrobromic acid, the layers were separated and the ether layer was dried over anhydrous sodium sulfate. On concentration of the ether solutions 1.1 grams (76%) of tris(o-tolyl)tin bromide were obtained which after recrystallization from methanol, melted at 98-99.5°C (lit. 99.5°C) (41). $^1\text{H-NMR}$ is consistent with known literature values (31).

PREPARATION OF TRISORTHOTOLYL TIN HYDRIDE (TOH)

Tris(o-tolyl)tin (TOH) has been prepared according to the method of Becker (41).



Starting Materials: Tris(o-tolyl)tin bromide was prepared as previously described. Lithium aluminum hydride and sodium potassium tartrate were used as supplied from Aldrich and Fisher, respectively. Diethyl ether was dried by storing over sodium wire.

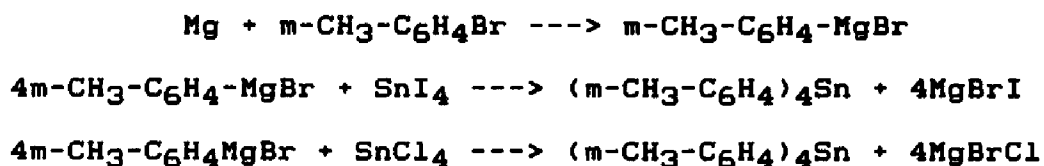
Apparatus: 250-mL 3-necked boiling flask, provided with a reflux condenser fitted with a calcium chloride tube, a dropping funnel and tube through which gaseous nitrogen could be introduced.

Procedure: The flask was dried thoroughly with a flameless heat gun while flushing with dry nitrogen. A solution of 1.1 grams of tris(o-tolyl)tinbromide dissolved in 25.0 milliliters of dry ether, was added dropwise to 2.0 grams of lithium aluminum hydride suspended in 50.0 milliliters of dry ether. After the addition, the

reaction mixture was stirred for three hours at room temperature. Water was carefully added until there was no further evidence of gas evolution. The contents of the flask were then poured into a solution of sodium potassium tartrate. The ether layer was separated, washed several times with water and dried over anhydrous sodium sulfate. The ether solution was then distilled at reduced pressure leaving a white solid melting at 90-94°C which after sublimation at 90°C gave a white product, melting at 95-97°C. Recrystallization from methanol gave 0.6 gram 65%, (lit. 77%), of white needles melting at 98-99°C (lit. 98.6-99.4°C) (41). ¹H-NMR showed a sharp signal at 405Hz. IR showed a sharp signal at 1270cm⁻¹, (38).

PREPARATION OF TETRAKISMETATOLYL TIN

Tetrakis(m-tolyl)tin has been prepared according to the method of Becker (41). The synthesis based on stannic chloride offered a higher yield, (50%), than stannic iodide, (32%).



Two recrystallizations from ethanol afforded feathery, pale yellow needles melting at 127-128.5°C (lit. 128.4-129.6°C) (41).

Starting Materials: Magnesium, 3-bromotoluene and stannic chloride were used as supplied from Aldrich. Stannic iodide was prepared as previously described. Benzene and tetrahydrofuran were distilled from calcium hydride and stored over sodium wire. Diethyl ether was dried by storing over sodium wire. Nitrogen gas was dried by passing through concentrated sulfuric acid.

Apparatus: 250-ml 3-necked boiling flask, provided with a reflux condenser fitted with a calcium chloride tube, a dropping funnel and tube through which gaseous nitrogen could be introduced.

Procedure: The flask was dried thoroughly with a flameless heat gun while flushing with dry nitrogen. A solution of 12.0 milliliters (0.099 mole) of 3-bromotoluene in 20.0 milliliters of dry tetrahydrofuran was added dropwise to a solution of 2.43 grams (0.1 mole) of magnesium in 40.0 milliliters of dry tetrahydrofuran. The flask was heated gently until the reaction began, after which heating was no longer necessary. After the addition, the reaction mixture was refluxed for one hour. A solution of 9.0 grams (0.0144 mole) of stannic iodide in 80.0 milliliters of dry benzene was added dropwise at room temperature to the reaction mixture. Upon completion of addition the reaction mixture was refluxed for two hours and then carefully hydrolyzed with 10% hydrobromic acid. The organic layer was separated, washed several times with water, and dried over anhydrous sodium sulfate. The mixed solvents were distilled at reduced pressure leaving a yellow, heavy, oily material which crystallized upon the addition of ethanol. When

stannic chloride was used in another experiment instead of stannic iodide and diethyl ether as a solvent instead of tetrahydrofuran, a yellow solid was formed instead of a yellow oil. Recrystallization twice from ethanol yielded 2.2 grams (32%) of pale yellow needles, melting at 126-128.5°C. When stannic chloride was used, there was a 50% yield of pale yellow needles melting at 127-128.5°C (lit. 128.4-129.6°C) (41). ¹H-NMR is consistent with known literature values (31).

PREPARATION OF TRISMETATOLYL TIN CHLORIDE

Tris(m-tolyl)tin chloride has been prepared according to the method of Kozeschkow (32).



Starting Materials: Tetrakis(m-tolyl)tin was prepared as previously described. Stannic chloride was used as supplied from Aldrich.

Apparatus: Oil bath, 250-mL round-bottom flask equipped with a reflux condenser, magnetic stirrer and mechanical stirrer.

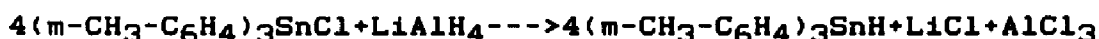
Procedure: Add 0.16 milliliters (1.36×10^{-3} mole) of stannic chloride to 2.1 grams (4.35×10^{-3} mole) of tetrakis(m-tolyl)tin in a 50-mL round-bottom flask fitted with a reflux condenser. It is not necessary for water to cool the condenser. The flask was placed in an oil bath whose temperature was slowly raised to 205°C.

The oil bath was heated at 200-210°C for three hours, followed by three hours at 155-160°C. The reaction vessel was allowed to cool to room temperature.

The solid mass was broken up and extracted with boiling ethanol. The filtrate was concentrated and cooled to form a yellow solid melting at 95-100°C. Recrystallization twice from ethanol yielded 1.0 gram (60%) of yellow needles melting at 106-108°C (lit. 108°C) (32). ¹H-NMR is consistent with known literature values.

PREPARATION OF TRISMETATOLYL TIN HYDRIDE (TMH)

Tris(m-tolyl)tin hydride (TMH) has been prepared according to the method of Becker (41).



Starting Materials: Tris(m-tolyl)tin chloride was prepared as previously described. Lithium aluminum hydride and sodium potassium tartrate were used as supplied from Aldrich and Fisher, respectively. Diethyl ether was dried by storing over sodium wire.

Apparatus: 250-mL 3-necked boiling flask, provided with a reflux condenser fitted with a calcium chloride tube, a dropping funnel and tube through which gaseous nitrogen could be introduced.

Procedure: The flask was dried thoroughly with a flameless heat gun while flushing with dry nitrogen. A solution of 1.0 gram of tris(m-tolyl)tin chloride in 40.0 milliliters of dry ether, was added dropwise to 2.0 grams of lithium aluminum hydride suspended in 50.0 milliliters of dry ether. After completion of the addition, the reaction mixture was stirred for three hours at room

temperature. The water was carefully added until there was no further evidence of gas evolution. The contents of the flask were then poured into a solution of sodium potassium tartrate. The ether layer was separated, washed several times with water and dried over anhydrous sodium sulfate. The ether solution was then distilled at reduced pressure to give a yellow viscous oil. This oil was vacuum distilled to yield a yellow liquid. On exposing this yellow liquid to air, it became a yellow viscous material. $^1\text{H-NMR}$ showed a sharp signal (Sn-H) at 414Hz.

B - Techniques

1 - The ESR Spectrometer

The spectra were taken with a Varian E-9 ESR spectrometer using 100 KHz field modulation fitted with an E-231 multi-purpose cavity (TE₁₀₂ rectangular) and an E-257 variable temperature accessory. X-band frequencies were measured using a model 5248L Hewlett-Packard frequency counter with 5255-A GHz insert. ESR spectra were calibrated using an O.S. Walker Model G502 NMR proton gaussmeter.

2 - The Cold Temperature Cell

Two types of low temperatures experiments were performed. At temperatures of 93°K and higher the Varian variable temperature dewar was used. The sample was cooled by the flow of nitrogen gas from vaporized liquid nitrogen. Temperatures were controlled to $\pm 1^\circ\text{K}$ and were determined by measuring the voltage output of an iron-constantan thermocouple using an ESI Model 300 Potentiometric Voltmeter Bridge.

At temperatures between 4°K and 60°K an Air-Products Cyro-Tip Model LTD-3-110 liquid transfer Heli-Tran system was used. The sample was cooled by the flow of helium gas from vaporized liquid helium. The sample temperature was controlled to $\pm 0.1^\circ\text{K}$. Temperatures were determined by measuring the voltage output from a chromel vs. gold thermocouple using an ESI Model 300 Potentiometric Voltmeter Bridge.

3 - Purification of Solvent

Reagent grade 2-methyltetrahydrofuran was purified by refluxing over night over sodium wire, redistilling and storing over sodium-potassium alloy and benzophenone under vacuum. 2-methyltetrahydrofuran was frozen and degassed several times under vacuum. At this point, the blue color of the benzophenone radical developed in the vicinity of the metal alloy. Degassed 2-methyltetrahydrofuran was condensed into the reaction vessel under vacuum.

2-methyltetrahydrofuran forms a rigid glass matrix at liquid nitrogen temperatures and possesses several important properties (42) such as:

1. Optical transparency;
2. Rigidity and non-cracking matrix;
3. The ability to dissolve a reasonable quantity of solute;
4. Not readily photolyzed or easily capable of producing free radicals under visible light.

Reagent grade n-pentane was purified by refluxing over night over sodium wire, redistilling and storing over sodium.

4 - Light Source

The light output of a 1.6 Kw Oriel Hg-Xe lamp was filtered using a water filter followed by a pyrex glass filter. The filtered light was focused upon the irradiation slits of the cavity by a spectro-sil quartz lens. A 5 cm. water filter with quartz windows was inserted in the optical train to absorb infrared radiation and prevent localized heating of the sample. It was followed by a pyrex glass filter to remove ultraviolet irradiation (100% transmission above 350 nm, 0% transmission below 320 nm).

5 - Sample Preparation

Triaryltin radicals were generated three different ways:

(A) through low temperature sodium-potassium reduction of parent compounds; (B) through low temperature peroxide oxidation of parent hydride; (C) through photolysis of cyclopentadienyl precursors.

A - Sodium-potassium alloy experiments

Solvents: Reagent grade 2-MTHF was purchased from Aldrich and purified as previously described.

Reagents: Pure sodium and potassium metal were cleaned under mineral oil. Accurate quantities of sodium and potassium wire were obtained by cutting off measured lengths under mineral oil followed by washing the metal using petroleum ether. Isotopically enriched tetraphenyltin, tetrakisorthotolytin, trisorthotolytin iodide, hexakisorthotolylditin and tetrakisparatolytin were prepared as previously described in section IIIA.

Preparation of triaryltin anions: The triaryltin anion solutions for optical spectroscopy were prepared using sodium-potassium alloy (43-46). In specially designed reaction vessels under high vacuum, (figure 4A), approximately 0.01 gram of the solid sample was placed into the bottom of the reaction vessel followed by equal quantities of sodium and potassium in the side-arm of the sample tube. The reaction vessel and its contents were then thoroughly degassed under high vacuum (10^{-5} - 10^{-6} torr), (figure 4B), several times. The sodium-potassium mixture was flame heated strongly at the side arm to form a clean alloy mirror at the top-side arm of the sample tube. Impurities associated with the alkali metals were trapped at the bottom of the side-arm and were sealed off. About one milliliter of dry, degassed 2-MTHF was condensed into the sample tube under vacuum.

The sample tube was sealed from the top and removed from the vacuum line (figure 4C). Triphenyltin anions were generated by reaction of the parent compounds in solution with the sodium-potassium alloy as indicated by the formation of a yellow solution. As an independent check on the formation of triphenyltin anions, the NMR spectra of the products were obtained, they were identical in the line shape and line position with the results reported by Bramwell (5) and Cox (47).

Figure 4A - A schematic diagram of a reaction vessel.

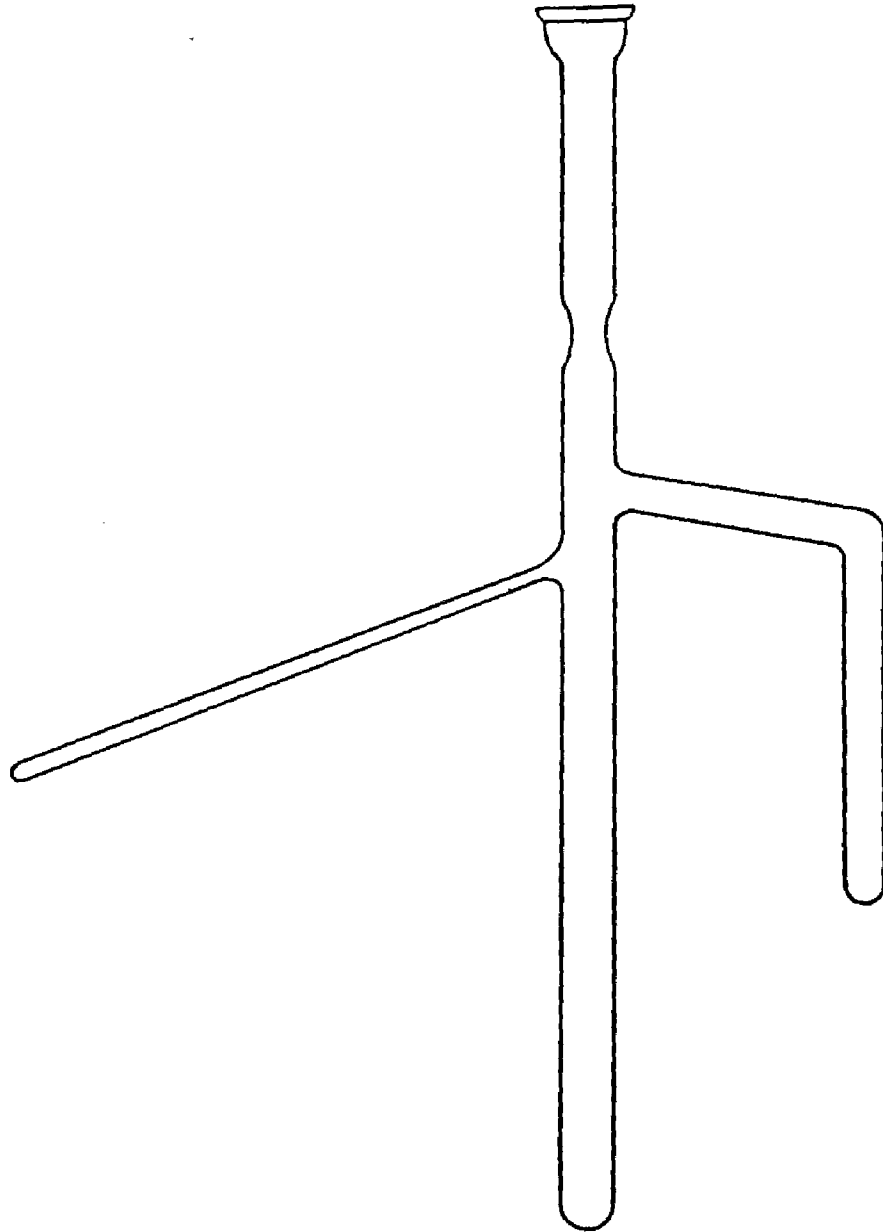


Figure 4B - A schematic diagram of a reaction vessel
under the vacuum line.

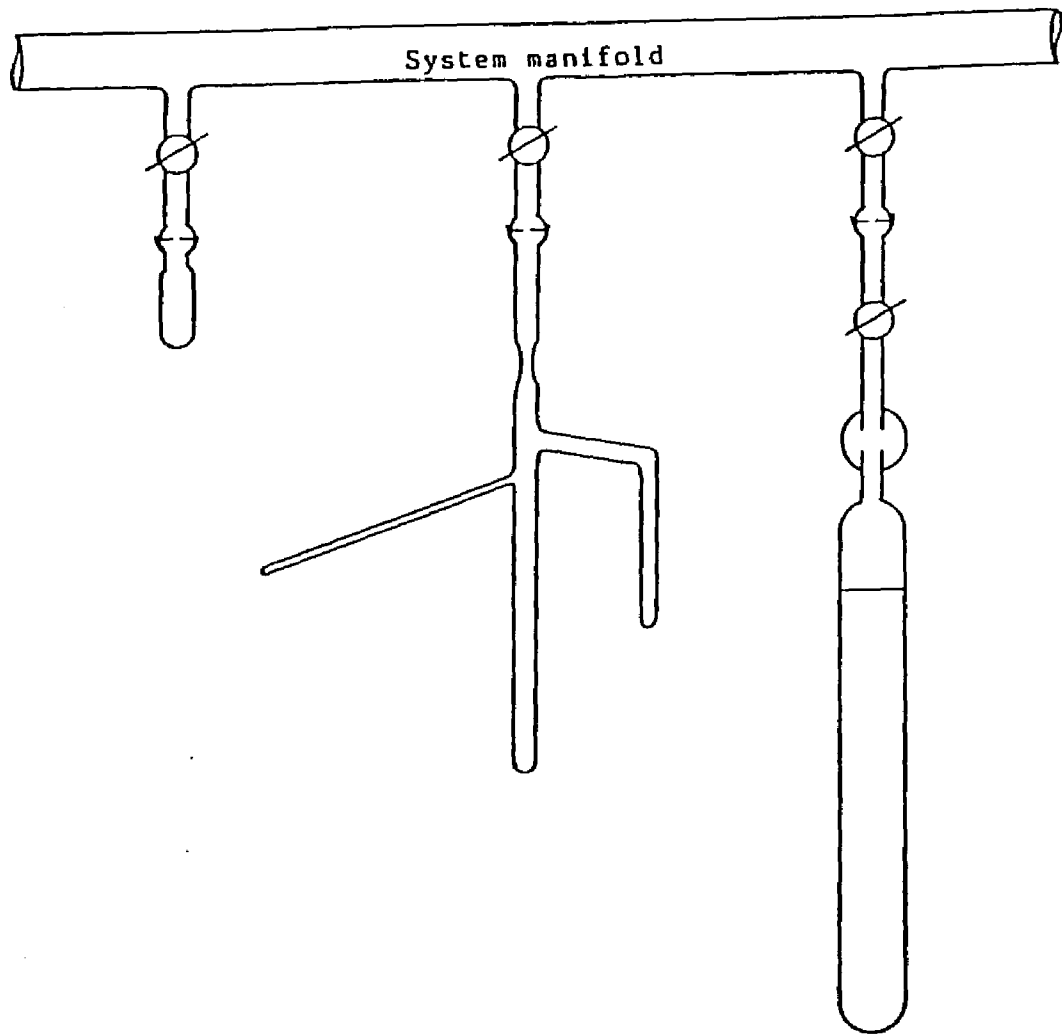
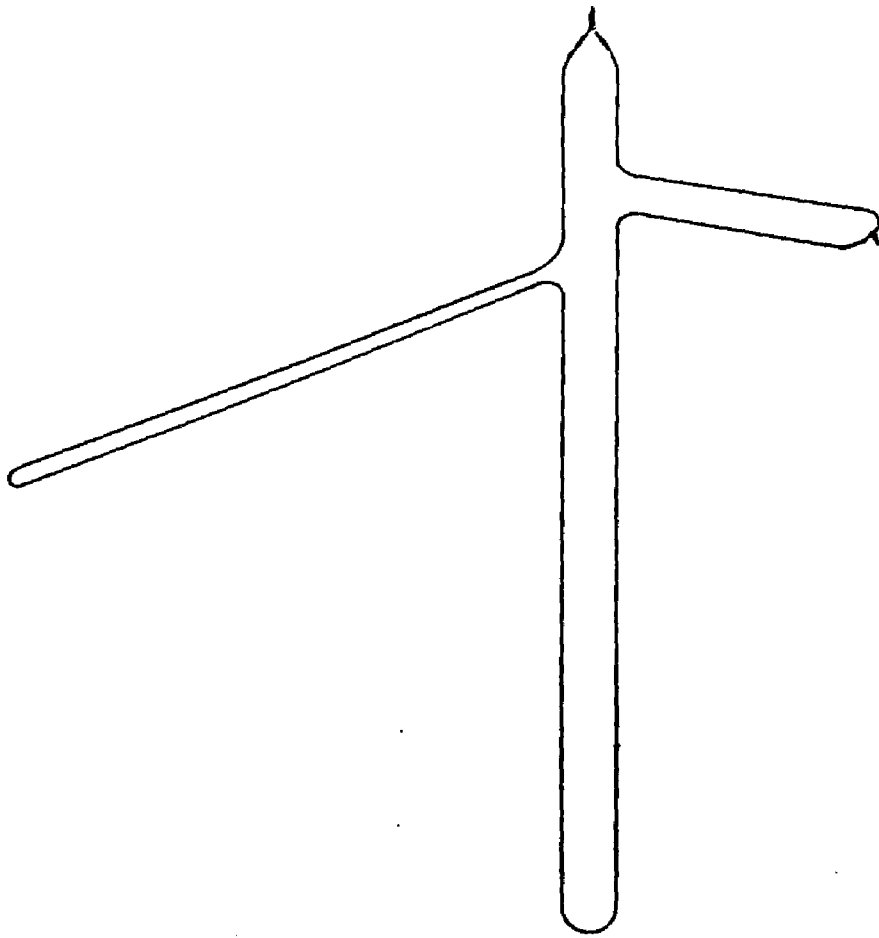


Figure 4C - The reaction vessel removed from the vacuum line.



Special care was taken not to keep the solution in contact with the sodium-potassium alloy for long periods of time. If triphenyltin anion solutions are kept in contact with sodium-potassium alloy for long periods of time a reddish-brown color is formed. This color may indicate undetermined polymerization, dianion formation or synthesis of hexa-arylditin.

Although the reduction of tetraphenyltin, hexa-phenylditin and triphenyltin chloride by sodium or potassium metal has been reported (5, 30, 48-51) the use of pure sodium or potassium mirrors failed to provide sufficiently concentrated aryltin anions for detailed analysis of radical spectra.

B - t-Butyl Peroxide Experiments

The following compounds were used to produce triaryltin radicals through t-butyl peroxide oxidation of aryltin hydrides: triphenyltin hydride, tris (o-, m-, p-tolyl)tin hydrides.

Solvents: Reagent grade n-pentane was purchased from Fisher and purified as previously described.

Reagents: Di-t-butyl peroxide was used as supplied from Aldrich. Natural abundance, triphenyltin hydride, trisparatolytin hydride trismetatolytin hydride and trisorthotolytin hydride were prepared as previously described in section III-A. A 0.2M solution of di-t-butyl peroxide in n-pentane and a 0.4M solution of triaryl tin hydride in n-pentane were prepared. Solutions were mixed and transferred by pipet to a quartz ESR tube, flushed thoroughly with dry nitrogen gas for two minutes, and sealed quickly (7).

C - Cyclopentadienyl Experiments

Solvent: Reagent grade 2-MTHF was purchased from Aldrich and purified as previously described.

Reagent: Triphenyl-1-cyclopentadienyln tin was prepared as previously described in section III-A. A 0.01M solution of triphenyl-1-cyclopentadienyln tin in 2-MTHF was prepared, transferred by pipet to a quartz ESR tube, flushed thoroughly with dry nitrogen gas for two minutes, and sealed quickly.

IV. RESULTS

A - TETRAPHENYLTIN

1. Anion synthesis

Triphenyltin anions were generated using the alkali metal reduction of tetraphenyltin in 2-methyltetrahydrofuran.

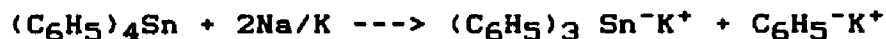
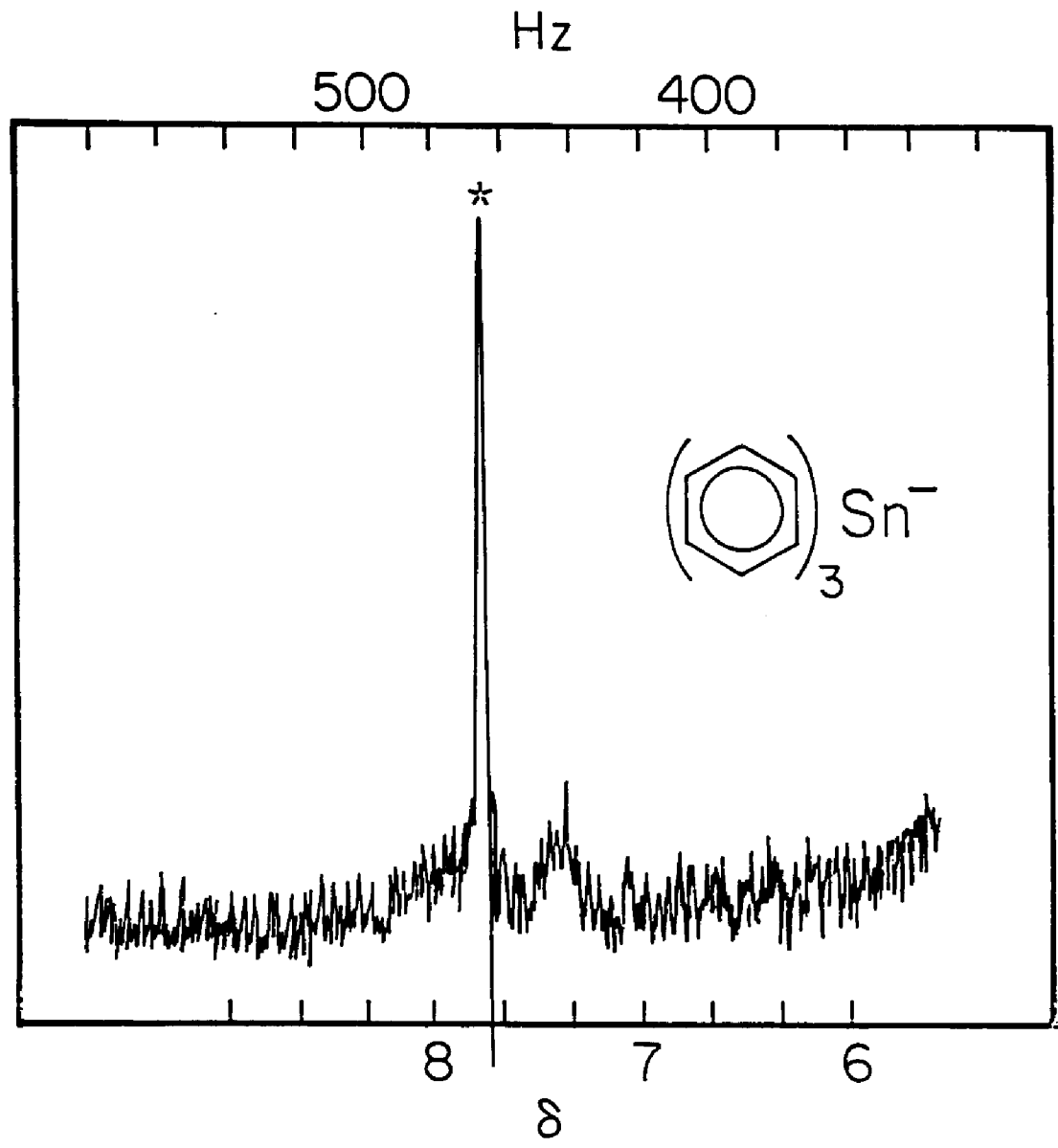


Figure 5 shows the proton NMR spectra of the products. The spectra were identical in line shape and line position with the results reported by Bramwell (5) and Cox (47), and thus serve as an independent check of the experimental method. The peak marked with a star has been identified as the benzene resonance and occurs in the tetraphenyltin reduction, as expected.

Radicals were generated using the focused filtered light output of a 1.6 kW Oriel medium pressure Hg-Xe lamp. A water filter followed by a pyrex glass filter produced 100% transmission at wave lengths greater than 350 nm and less than 700 nm. The parent compounds were

Figure 5 - 60 MHz ^1H -NMR Spectrum of $(\text{C}_6\text{H}_5)_3^{119}\text{Sn}^-$ obtained
by sodium-potassium reduction of $(\text{C}_6\text{H}_5)_4\text{Sn}$
in 2-MTHF.



isotopically enriched to 84% ^{119}Sn with 16% of other tin isotopes in natural abundance.

2. ESR Spectra

Low temperature experiments were performed at 93°K and 4°K. The experimental spectra at 4°K were similar to those at 93°K. The only differences were characteristic Boltzmann enhancements of signal intensity.

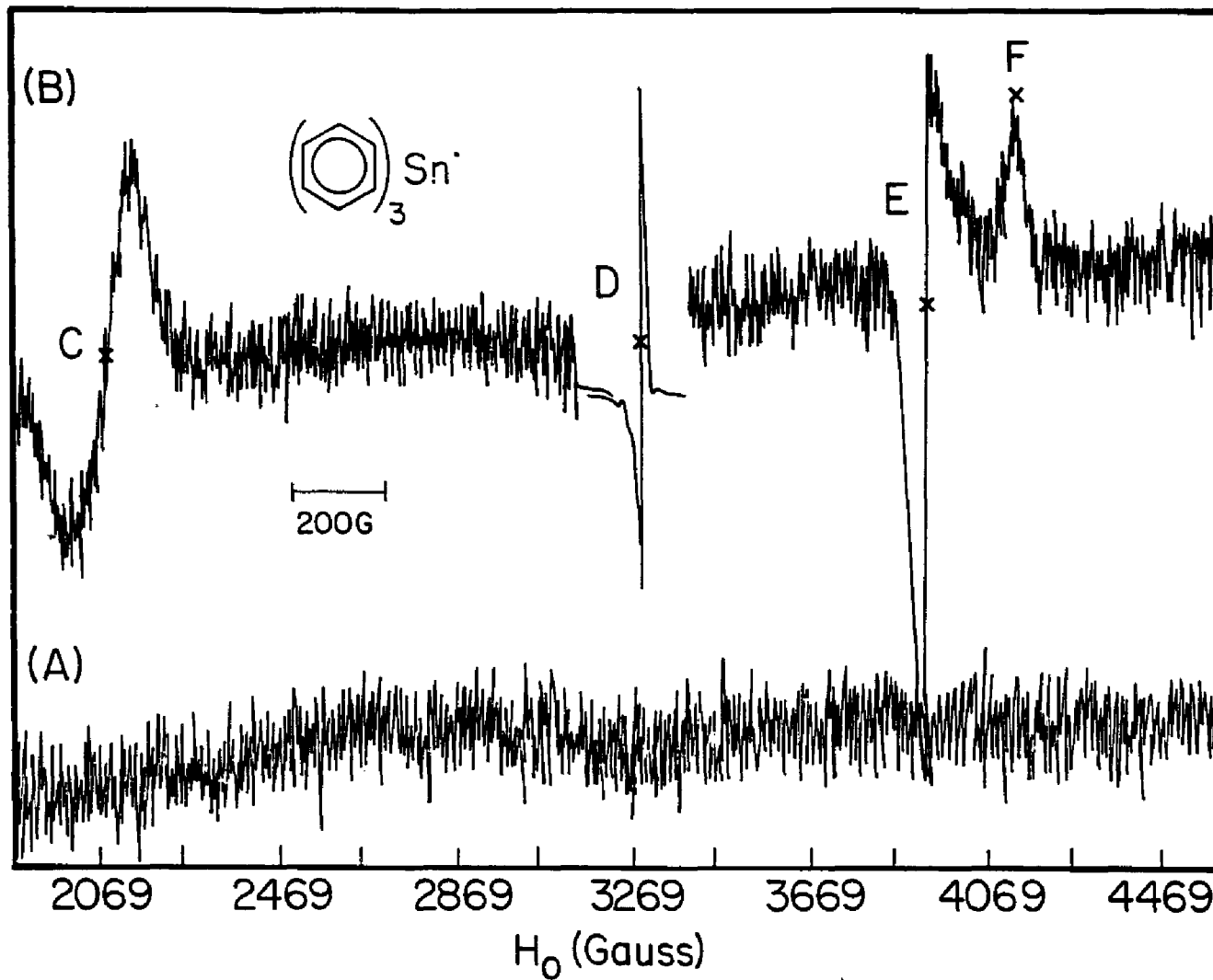
The visible light dependence of 2-MTHF was determined by running a neat sample of 2-MTHF and Na/K alloy under the experimental conditions before and after exposing it to the focused light source. No ESR signal was observed indicating that no detectable radical concentrations were present.

Figure 6 consists of two parts: figure 6A and figure 6B. Figure 6A is the base line which is obtained by running the sample under the experimental conditions before exposing it to a focused light source.

Figure 6B shows the ESR spectrum of the triphenyltin radical at 93°K. The spectrum has a Gaussian line shape and consists of three main features:

Figure 6 - The ESR spectra of $(C_6H_5)_3^{119}Sn$ in 2-MTHF at 93 K.

- (A) Base line - sample in place but not irradiated.
- (B) Visible light irradiation of sample producing spectral features C, D, E, F.



1. Signal C: a down-field (2117 G) broad signal of 150 G line-width;
2. Signal D: a central signal (3269 G) of high intensity and 14 G line-width;
3. Signals E, F: a pair of signals at high-field (3913, 4112 G) of 50 G and 30 G line-width. These two signals were separated by 200 G.

As the spectra show in figure 6B, signal C has a first derivative Gaussian line shape and is about 1152 G from signal D (central signal). The broadened signal (150 G peak-to-peak width) suggests that there may be unresolved structure.

Signal D (3269 G) of the triphenyltin radical has a line-width of 14 G. The high intensity of this peak may be due to a combination of undetermined polymerization, dianion formation, and the formation of radical from the 16% abundance of other tin isotopes in the parent anion.

At high-field, signal E which is observed at 3913 G is sharp and has a first-derivative line shape with a line-width of 50 G. This signal is assigned as the A_{\parallel} or A_{xy} hyperfine coupling by analogy to Lehnig (6) and to

Berclaz (4). Signal F at 4112 G is broad and has an absorption line shape with a line-width of 30 G (half-width at half-height). This signal is assigned as the A_{\parallel} or A_z hyperfine coupling. The isotropic and anisotropic hyperfine splittings were determined using equations (21-22) in section II where $a_{iso} = 1/3(A_{\parallel} + 2A_{\perp})$. Table 1 shows that isotropic and anisotropic hyperfine splitting are in excellent agreement with those reported by Berclaz (4).

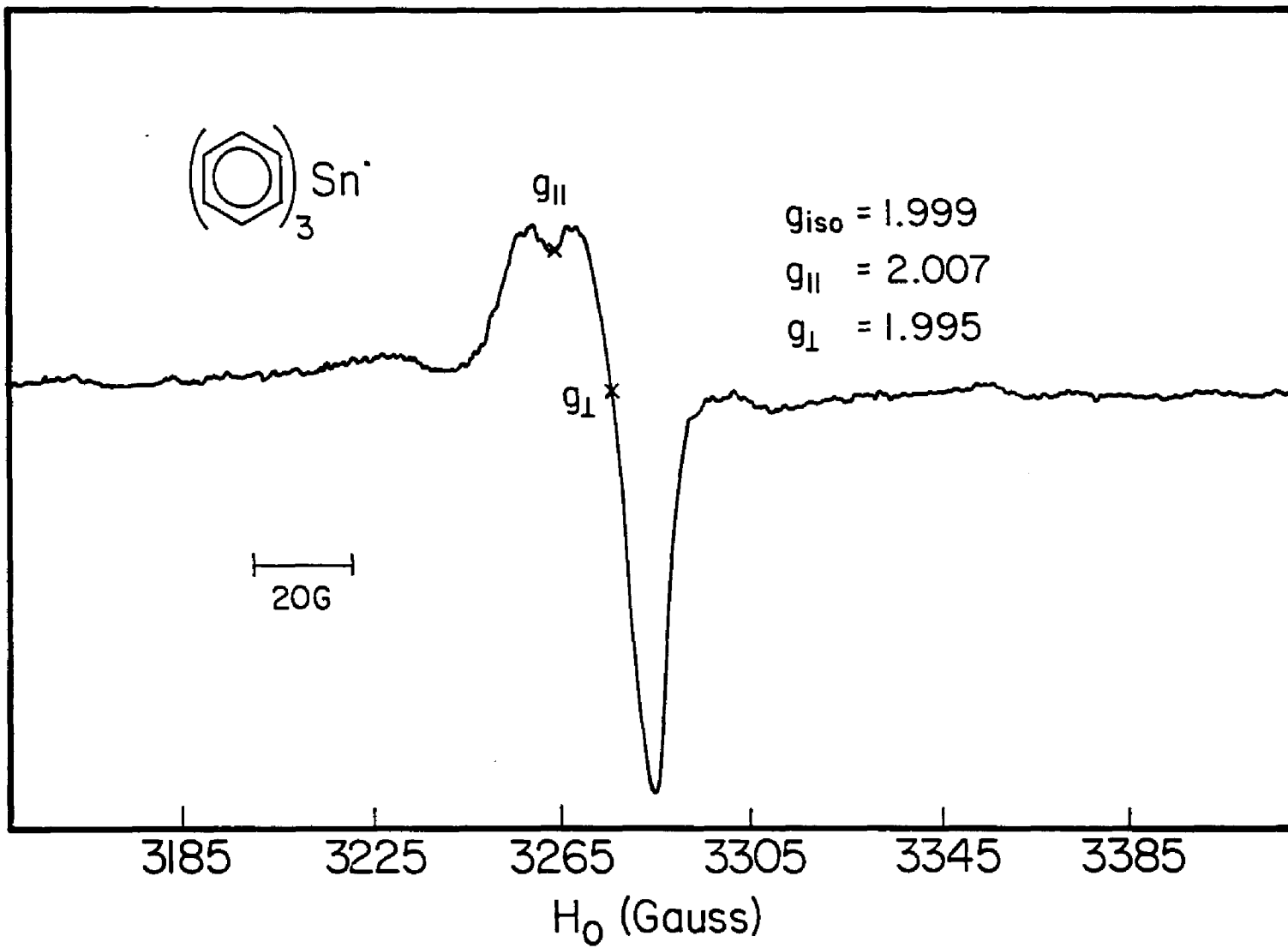
Axially symmetric g tensors for randomly oriented radicals, are known to give asymmetric line shapes with a shoulder corresponding approximately to g_{\parallel} and a stronger maximum corresponding to g_{\perp} . The stronger absorption in the region of g_{\perp} is due to the greater probability in randomly oriented samples of observation of molecules with the g_{\perp} orientation (17).

Figure 7 shows the complex spectrum of the central signal D. No $g = 2$ signal is expected from parent anion compounds based on ^{119}Sn . The origin of signal D, therefore, is uncertain, and may be the result of partial decomposition of the sample, parent compounds based on the 16% abundance of the tin isotopes, or dianion formation.

Figure 7 - The ESR spectra of the central signal at $g = 2$
of $(C_6H_5)_3^{119}Sn$ in 2-MTHF at 93 K.

$$A = g_{\perp}$$

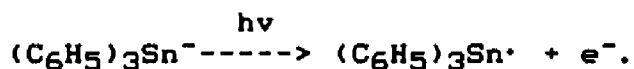
$$B = g_{\parallel}$$



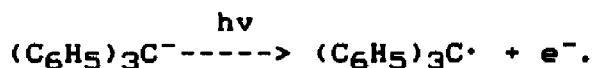
The determination of g-factors was based on the spectra of ^{120}Sn based parent compounds. It was reasonably assumed that the g-factor for ^{120}Sn would be identical to that of ^{119}Sn . g-Factor values are listed in table 2.

The ESR signal of the triphenyltin radical is light independent. The irradiation time required to generate sufficient triphenyltin radicals to obtain a signal to noise ratio of 6:1 is about 3 - 5 minutes. It is apparent that as long as the sample is exposed to the light source the signal intensity will increase. When the light source was removed the signal intensity did not change.

Warming of the trapped radical from 93°K to 103°K , slightly above the melting point of the matrix, caused the signal intensity to decrease to zero. On recooling to 93°K , the signal did not return until the sample was irradiated again. These results are consistent with a mechanism which assumes the generation of triphenyltin radical by the photo-oxidation of triphenyltin anion according to the following reaction (5):



These results are analogous to those reported for triphenylmethyl radical (52):



3. Hyperfine Splittings and g-Factor Determination

The results of analyses of the ESR spectra for triphenyltin radical are shown in tables 1, 2 and 3. As seen in figure 6B, the hyperfine splitting is not symmetrically placed about the central signal D. The spectra are, therefore, far from first order in appearance and the hyperfine coupling constant is not simply the separation of the high-field, (signals E, F) and low field (signal C) spectral features. Accurate values can only be obtained by application of the Breit-Rabi equation (17-20) (equation 35-37, sec. II).

The g values for the ^{119}Sn based anion, (signal D), were estimated using a trial value obtained from natural abundance ^{120}Sn . From that g value, H_0 was calculated and used in the Breit-Rabi equation to determine the hyperfine splitting.

From an analysis of figure 6B, the magnetic fields associated with the signals E and F are 3913 G and 4112 G, respectively. The field at signal D is estimated at 3269 G. Applying these data to equations (35-37) in section II, the isotropic and anisotropic hyperfine splittings are:

$$a_{iso} = 1823 \text{ G}$$

$$\tau_{\parallel} = 457 \text{ G}$$

$$A_{\parallel} = 2280 \text{ G}$$

$$A_{\perp} = 1594 \text{ G}$$

From these data and through the use of equations (35-37) it was possible to calculate the line position of the low-field spectral features. The results are in excellent agreement with the observed data and are shown in table 4.

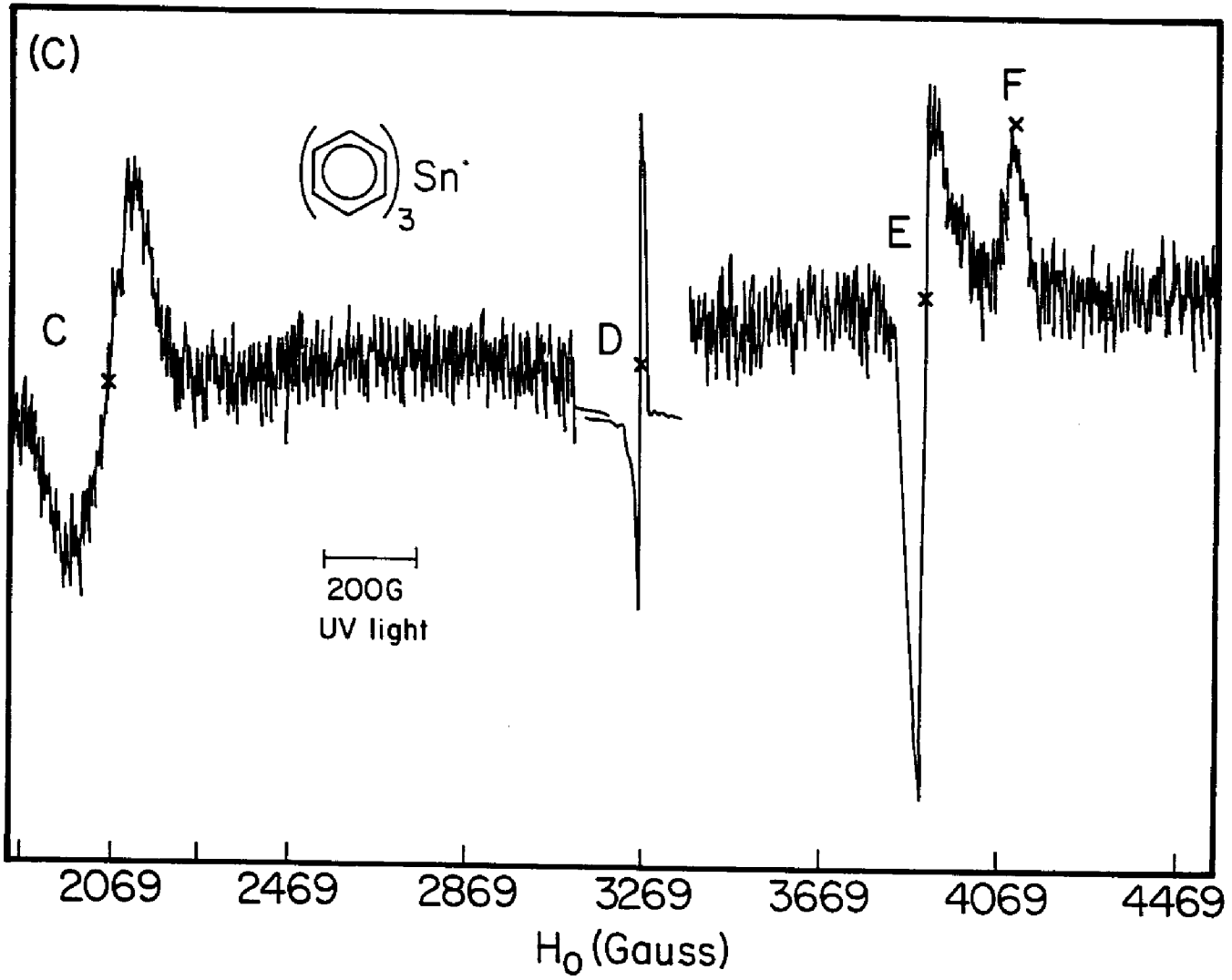
Equations (29-33) in section II were used to estimate the percent of "S" and "P" character of the orbital containing the unpaired electron (14), the extent of hybridization, the out-of-plane angle, θ , (the complement of the ligand-tin-symmetry axis angle), and the ligand-tin-ligand bond angle, ξ . These calculations are based on atomic parameter calculations of Morton and Preston (22).

4. Ultraviolet (UV) Degradation

Triphenyltin radicals were generated using unfiltered UV light. Figure 6C shows the ESR spectrum of the UV irradiated triphenyltin radicals in a 2-MTHF glass at 93 K.

The high and low-field spectral features were identical in line shape and line position with results observed using visible light, (see figure 6B). The intensity of the central signal was dramatically enhanced by UV irradiation. It was observed that 2-MTHF produces free radicals under UV irradiation, and most probably contributes significantly to the line shape and line position of signal D.

Figure 6C - The ESR spectra of UV irradiated
 $(\text{C}_6\text{H}_5)_3^{119}\text{Sn}$ in 2-MTHF at 93 K.



Radical	a_{iso}	τ_{\perp}	A_{\parallel}	A_{\perp}	g_{\parallel}	g_{\perp}
$Ph_3Sn\cdot$	1823	229	2280	1594	2.007	1.995
		$\bar{\xi} = 114.6^\circ$		$\theta = 13.6^\circ$		
$Ph_3Sn\cdot(4)$	1866	234	2334	1632	2.007	1.995
		$\bar{\xi} = 114.6^\circ$		$\theta = 13.6^\circ$		

Table 1 - Hyperfine splitting and g-factor parameters for triphenyltin radical.

where a_{iso} is the isotropic hyperfine splitting, τ_{\perp} is the anisotropic hyperfine splitting, A_{\perp} and A_{\parallel} are the hyperfine splitting for a magnetic field oriented perpendicular and parallel to the symmetry axis, g_{\perp} and g_{\parallel} are the g-factor values for a magnetic field oriented perpendicular and parallel to the symmetry axis, $\bar{\xi}$ is the ligand-tin-ligand inter-bond, and θ is the out-of-plane angle, (the complement of the ligand-tin-symmetry axis angle).

		(p-CH ₃ -C ₆ H ₄) ₃ Sn·	(C ₆ H ₅) ₃ Sn·	(o-CH ₃ -C ₆ H ₄) ₃ Sn·
A	G	2387	2280	2551
A _⊥	G	1644	1594	1811
a _{iso}	G	1891	1823	2058
τ	G	495	457	493
C ² _s		0.121	0.117	0.132
C ² _p		0.953	0.879	0.948
C ² _s +C ² _p		1.074	0.996	1.080
C ² _p /C ² _s		7.86	7.53	7.20
g _⊥		1.998	1.995	1.998
g		2.005	2.007	2.006
g _{iso}		2.000	1.999	2.001
̄ (deg)		114.8	114.6	114.4
θ (deg)		13.4	13.6	13.9

TABLE 2- ESR Parameters for Triaryltin Radicals.

A₀=15600* G

2B₀=520* G

* Morton and Preston atomic parameters (22).

Radical	Coupling					
	Constants	C_S^2	C_P^2	λ^2	Ξ	θ
Ph ₃ Sn·	$a_{iso} = 1823$ G $\tau = 457$ G	0.117	0.879	7.53	114.6°	13.6°

Table 3 - "S" and "P" character of the central atom for Ph₃Sn· in 2-methyltetrahydrofuran at 93° K.

$$C_S^2(\text{S-character}) = a_{iso}/A_0$$

$$C_P^2(\text{P-character}) = \tau_{||} / 2B_0$$

where A_0 and B_0 are theoretical isotropic and anisotropic coupling constants of 15600 G and 520 G, respectively (22). a_{iso} and $\tau_{||}$ are respective experimental isotropic and anisotropic coupling constants.

$$\lambda^2(\text{hybridization}) = C_P^2/C_S^2$$

$$\Xi = \cos^{-1} \left[\frac{1.5}{2\lambda^2 + 3} - \frac{1}{2} \right]$$

$$\cos^2 \theta = \frac{1}{3} [1 + 2 \cos \Xi]$$

where Ξ is the ligand-tin-ligand inter-bond angle, and θ is the out-of-plane angle, (the complement of the ligand-tin-symmetry axis angle).

where A_{\perp} , and A_{\parallel} are the hyperfine splitting values for a magnetic field oriented perpendicular and parallel to the symmetry axis. a_{iso} , and τ_{\perp} are the isotropic and anisotropic hyperfine splitting respectively. C_{s}^2 , and C_{p}^2 are "S" and "P" character, respectively. (λ^2) C_{p}^2/C_{s}^2 is the hybridization ratio. g_{\perp} and g_{\parallel} are respectively, the g values for a magnetic field oriented perpendicular and parallel to the symmetry axis. $\bar{\alpha}$, θ are respectively, the ligand-tin-ligand inter-bond angle, and out-of-plane angle, (the compliment of the ligand-tin-symmetry axis angle).

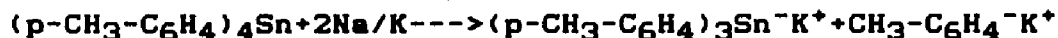
	H_k	H_k	H_o	H_1	H_1
Observed $(C_6H_5)_3Sn^{\cdot}$		2117	3269	3913	4112
Calculated	1516	2218	3267/3272	3913	4112
Observed $(p-CH_3-C_6H_4)_3Sn^{\cdot}$		2083	3273	3930	4140
Calculated	1420	2175	3266/3273	3930	4140
Observed $(o-CH_3-C_6H_4)_3Sn^{\cdot}$		1942	3260	3971	4166
Calculated	1151	2009	3250/3262	3971	4166

Table 4 - Observed and calculated triaryltin radical ESR line positions calculated using Breit-Rabi equation (17-20).

B - TETRAKISPARATOLYLtin

1. Anion synthesis

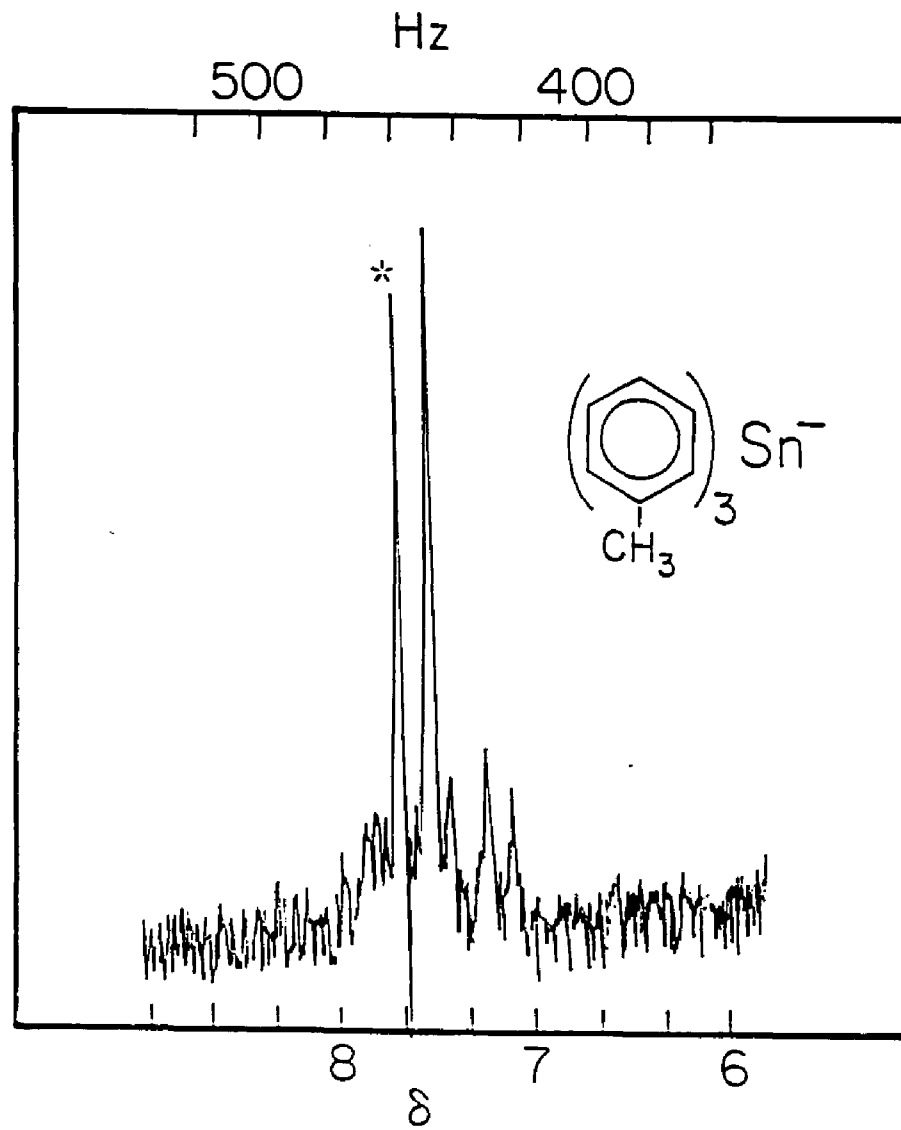
Triparatolytin anions were generated using the alkali metal reduction of tetrakisparatolytin in 2-methyltetrahydrofuran.



The proton NMR spectra of the products are shown in figure 8. The spectra were similar in line shape with the results reported by Bramwell (5) and Cox (47) for the triphenyltin anion, and strongly suggested the formation of the triparatolytin anion. The peak marked with a star has been identified as the toluene resonance .

Radicals were generated using the focused filtered light output of a 1.6 kW Oriel medium pressure Hg-Xe lamp in an identical manner to triphenyltin radicals. The parent compounds were isotopically enriched to 84% ^{119}Sn with 16% of other tin isotopes in natural abundance.

Figure 8 - 60 MHz ^1H -NMR Spectrum of $(\text{p-CH}_3\text{-C}_6\text{H}_4)_3^{119}\text{Sn}^-$
obtained by sodium-potassium reduction of the
 $(\text{p-CH}_3\text{-C}_6\text{H}_4)_4\text{Sn}$ in 2-MTHF.



2. ESR Spectra

Low temperature experiments were performed at 93°K and 4°K. The experimental spectra at 4°K were similar to those at 93°K. The only differences were characteristic Boltzmann enhancements of signal intensity.

Figure 9 consists of two parts: figure 9A and 9B. Figure 9A is the base line which is obtained by running the sample under experimental conditions before exposing it to a focused light source.

Figure 9B shows the ESR spectrum of the triparatolytin radical at 93°K. The spectrum has a Gaussian line shape and consists of three main features:

1. Signal C: a down-field (2060 G) broad signal of 160 G line-width.
2. Signal D: a central signal (3268 G) of high intensity and 16 G line-width.
3. Signals E, F: a pair of signals at high-field (3930, 4140 G) of 60 G and 30 G line-width. These two signals were separated by 210 G.

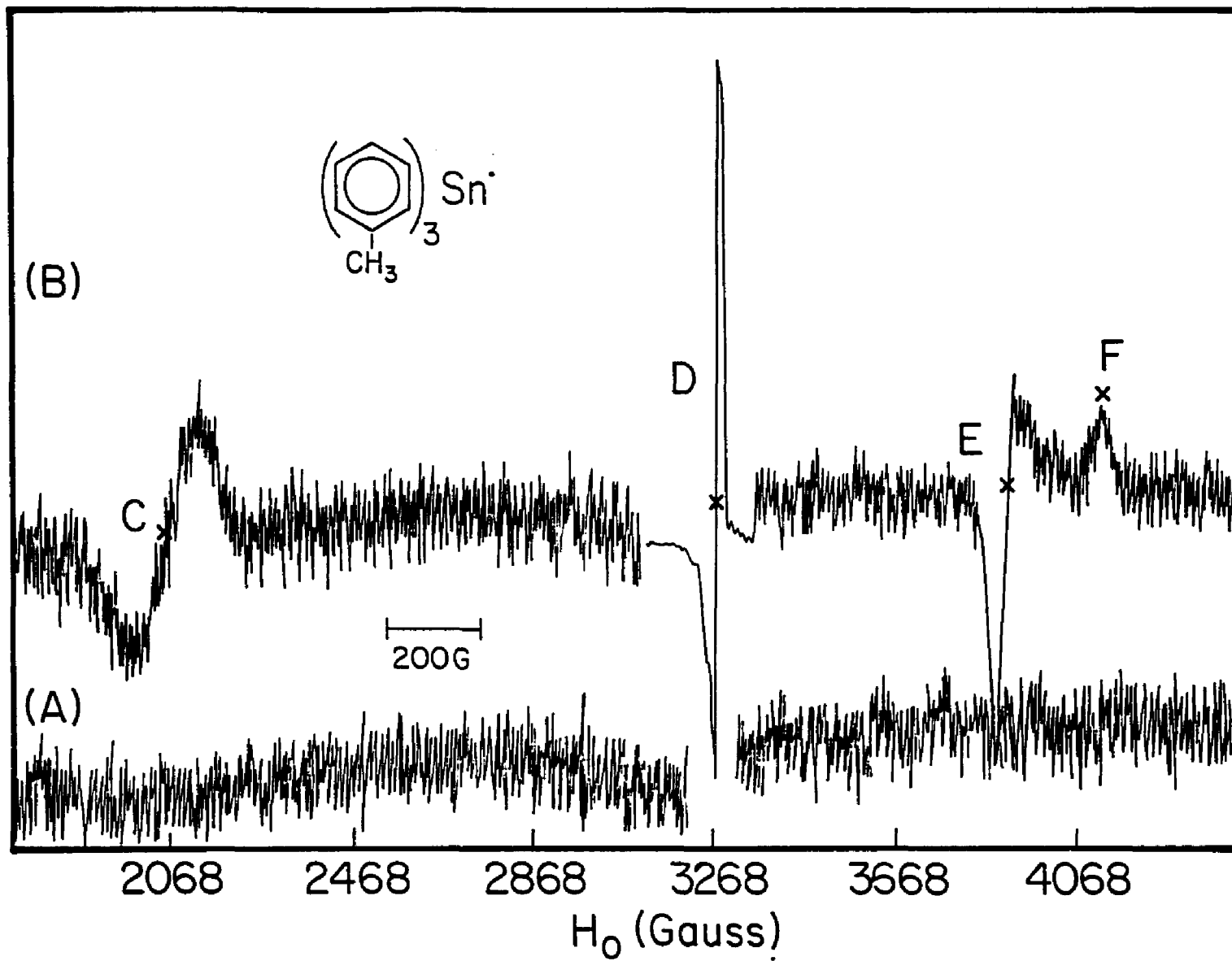
As the spectra show in figure 9B, signal C has a first derivative Gaussian line shape and is about 1200 G from signal D (central signal). The broadened signal (160 G peak-to-peak width) suggests that there may be unresolved structure.

Signal D (3268 G) of the triparatolytin radical has line-width of 16 G. The high intensity of this peak may be due to a combination of undetermined polymerization, dianion formation, and the formation of radical from the 16% abundance of other tin isotopes of the parent anion.

At high-field, signal E which is observed at 3930 G is sharp and has a first-derivative line shape with a line-width of 60 G. This signal is assigned as A_{\perp} or A_{xy} in an analogous manner to the triphenyltin radical. Signal F at 4140 G is broad and has an absorption line shape with a line-width of 30 G (half-width at half-height). This signal is assigned as A_{\parallel} or A_z hyperfine coupling. The isotropic and anisotropic hyperfine coupling constants are listed in table 2. These results are now reported for the first time.

Figure 9 - The ESR spectra of $(p\text{-CH}_3\text{-C}_6\text{H}_4)_3^{119}\text{Sn}$ in 2-MTHF at 93 K.

- (A) Base line - sample in place but not irradiated.
- (B) Visible light irradiation of sample producing spectral features C, D, E, F.



In an identical manner to the triphenyltin radical, signal A and B in figure 10 are assigned to the anisotropic g_{\perp} and g_{\parallel} , respectively. The g values (perpendicular and parallel) have been determined and their values are listed in table 2.

The ESR signal of the triparatolytin radical is light independent. The irradiation time required to generate enough triparatolytin radicals to obtain a signal to noise ratio of 6:1 is about 7 - 10 minutes. The light independent behavior of the triparatolytin radical was identical to that of the triphenyltin radical.

Warming of the trapped radical from 93°K to 103°K, slightly above the melting point of the matrix, caused the signal intensity to decrease to zero. On recooling to 93°K, the signal did not return until the sample was irradiated again. These results are consistent with a mechanism which assumes the generation of triparatolytin radical by the photo-oxidation of triparatolytin anion according to the following reaction:

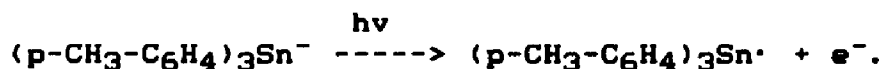
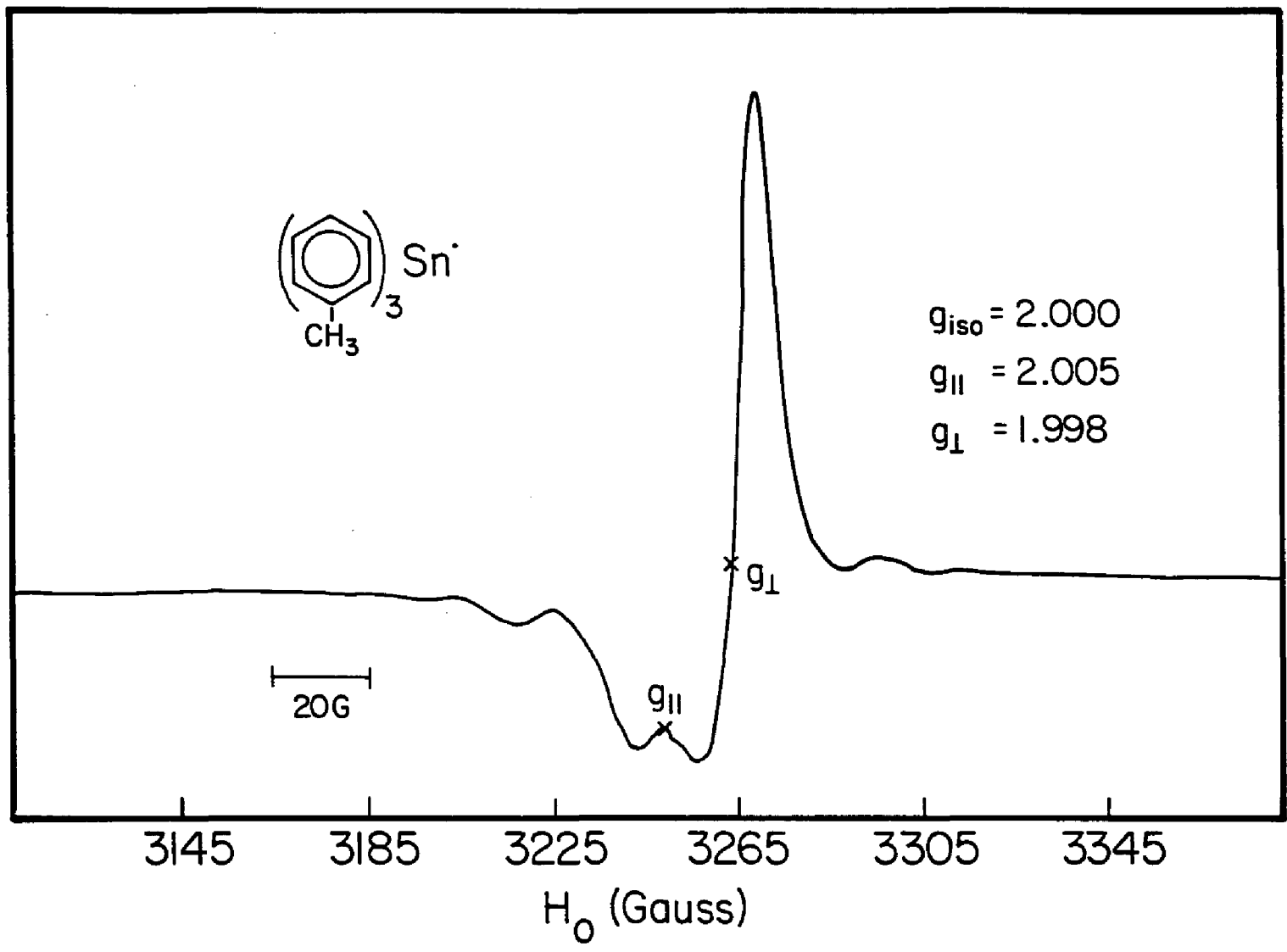


Figure 10 - The ESR spectra of the central signal at $g = 2$
of $(p\text{-CH}_3\text{-C}_6\text{H}_4)_3^{119}\text{Sn}$ in 2-MTHF at 93 K.

$$A = g_{\perp}$$

$$B = g_{\parallel}$$



3. Hyperfine Splittings and g-Factor Determination

ESR data for triparatolytin radical are listed in table 2. The isotropic and anisotropic hyperfine splitting were calculated from the high-field signals and signal D in an identical manner to that of triphenyltin radical.

From the analyses of signals E and F in figure 9B, the field associated with the first and second signals are 3930 G and 4140 G respectively. The field at the central signal D is estimated 3268 G. Applying these data in equations (35-37) in section II, the isotropic and anisotropic hyperfine are:

$$a_{iso} = 1891 \text{ G}$$

$$a_{||} = 495 \text{ G}$$

$$A_{||} = 2387 \text{ G}$$

$$A_{\perp} = 1644 \text{ G}$$

The spectra in figure 9B were identical in line shape with the spectra of the triphenyltin radical. Therefore, the position of signal C was derived in a similar manner. The calculated results are in excellent agreement with the observed values as shown in table 4.

4. Ultraviolet (UV) Degradation

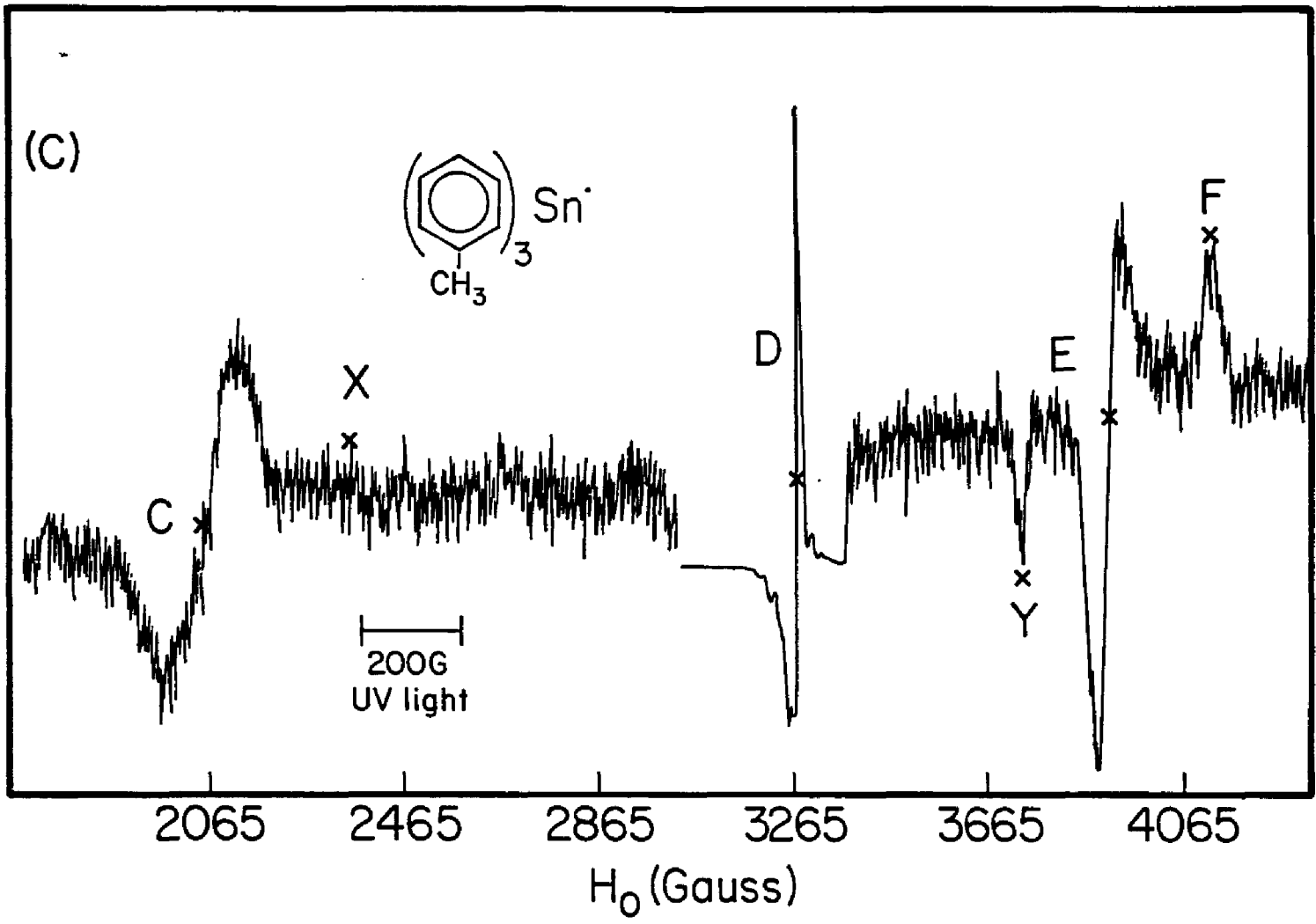
UV photolysis experiments were performed on the triparatolytin anion by simply removing the pyrex filter. Figure 9C shows the ESR spectrum of the UV irradiated triparatolytin radical at 93 K. The spectrum has a Gaussian line shape and consists of six main features: signals C, D, E, F, X, Y.

Signals C, E and F in figure 9B were identical in line shape and line position with the results observed in figure 9C. However, under UV irradiation two extra satellites are observed. At low-field, signal X (2265 G) is broad and has a first derivative Gaussian line shape and is about 1000 G from the central signal D ($g=2$). At high-field, signal Y which is observed at 3700 G is sharp, has an absorption line shape and is about 450 G from the central signal D. Signals X and Y are placed unsymmetrically about the central signal D. These results are consistent with a model which assumes UV degradation of triaryltin radicals.

The intensity of signal D of the UV irradiated triparatolytin radical has contributions from undetermined radical species and from the degradation of 2-MTHF

under UV light. A key problem in the UV photolysis is simultaneous production of undetermined radical species which complicate the identification of the triaryltin radical. These results strongly suggest photolytic degradation of the parent radical and the 2-MTHF matrix.

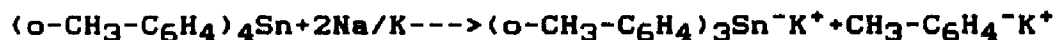
Figure 9C - The ESR spectra of UV irradiated
(p-CH₃-C₆H₄)₃¹¹⁹Sn· in 2-MTHF at 93 K.



C - TETRAKISORTHOTOLYLTIN

1. Anion synthesis

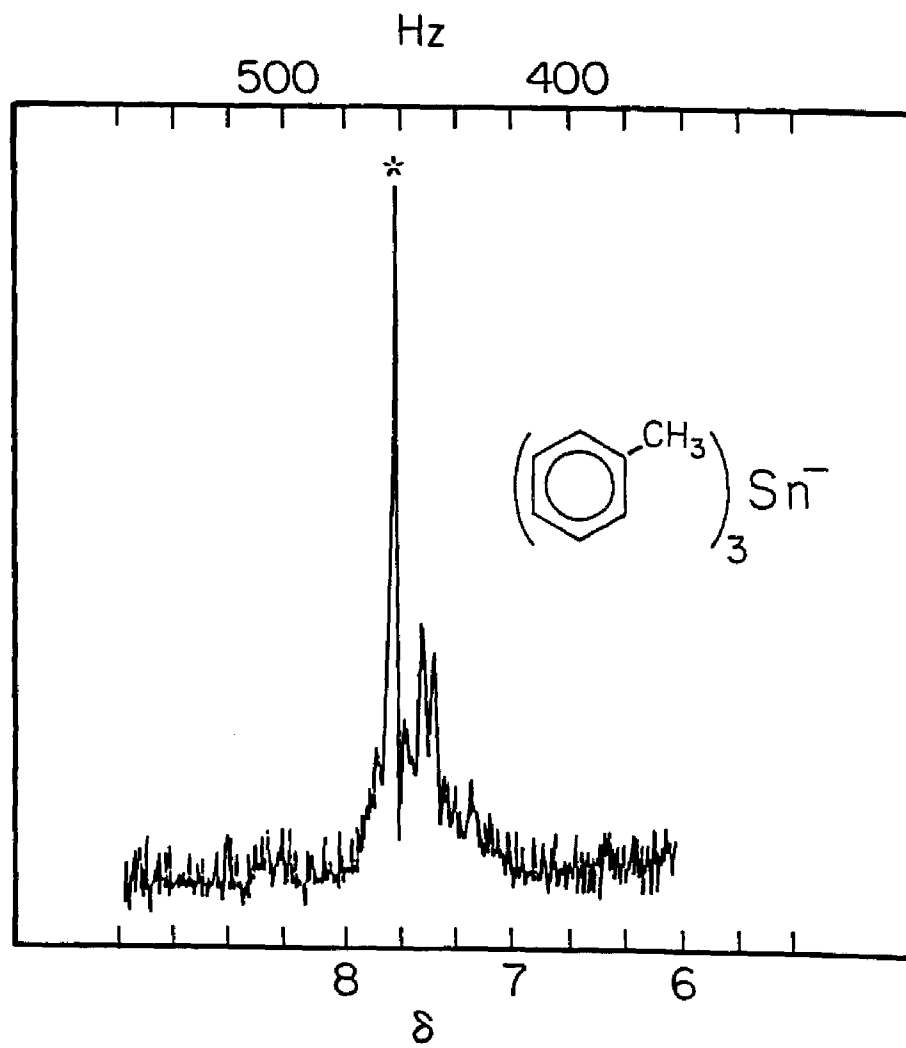
Triorthotolyltin anions were generated using the alkali metal reduction of tetrakisorthotolyltin in 2-methyltetrahydrofuran.



The proton NMR spectra of the products are shown in figure 11. The spectra were similar in line shape with the results reported by Bramwell (5) and Cox (47) for triphenyltin anion, and strongly suggested the formation of the triorthotolyltin anion. The peak marked with a star has been identified as the toluene resonance.

Radicals were generated using the focused filtered light output of a 1.6 kW Oriel medium pressure Hg-Xe lamp in an identical manner to triphenyltin radical. The parent compounds were isotopically enriched to 84% ^{119}Sn with 16% of other tin isotopes in natural abundance.

Figure 11 - 60 MHz ^1H -NMR Spectrum of $(o\text{-CH}_3\text{-C}_6\text{H}_4)_3^{119}\text{Sn}^-$
obtained by sodium-potassium reduction of the
 $(o\text{-CH}_3\text{-C}_6\text{H}_4)_4\text{Sn}$ in 2-MTHF.



2. ESR Spectra

Low temperature experiments were performed at 93°K and 4°K. The experimental spectra at 4°K were similar to those at 93°K. The only differences were characteristic Boltzmann enhancements of signal intensity.

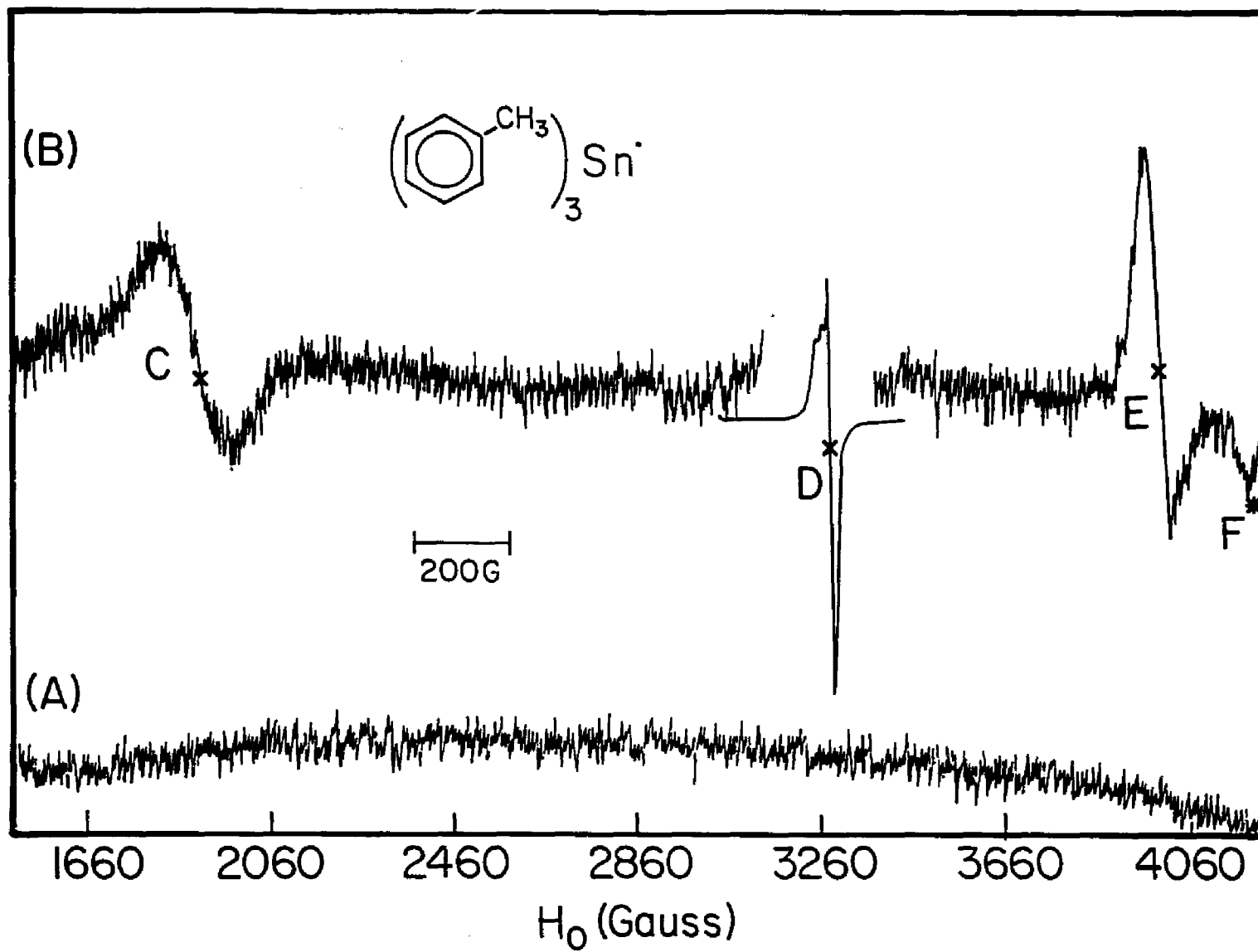
Figure 12 consists of two parts: figure 12A and 12B. Figure 12A is the base line which is obtained by running the sample under the experimental conditions before exposing it to a focused light source.

Figure 12B shows the ESR spectrum of the triorthotolytin radical at 93°K. The spectrum has a Gaussian line shape and consists of three main features:

1. Signal C: a down-field (1926 G) broad signal of 160 G line-width.
2. Signal D: a central signal (3260 G) of high intensity and 12 G line-width.
3. Signals E, F: a pair of signals at high-field (3971, 4166 G) of 60 G and 25 G line-width. These two signals were separated by 195 G.

Figure 12 - The ESR spectra of $(o\text{-CH}_3\text{-C}_6\text{H}_4)_3^{119}\text{Sn}$ in 2-MTHF at 93 K.

- (A) Base line - sample in place but not irradiated.
- (B) Visible light irradiation of sample producing spectral features C, D, E, F.



As the spectra show in figure 12B, signal C has a first-derivative Gaussian line shape and is about 1334 G from signal D (central signal). The broadened signal (140 G peak-to-peak width) suggests that there may be unresolved structure.

Signal D (3260 G) of the triorthotolytin radical has a line width of 12 G. The high intensity of this peak is due a combination of undetermined polymerization, dianion formation, and the formation of radical from the 16% abundance of other tin isotopes of the parent anion.

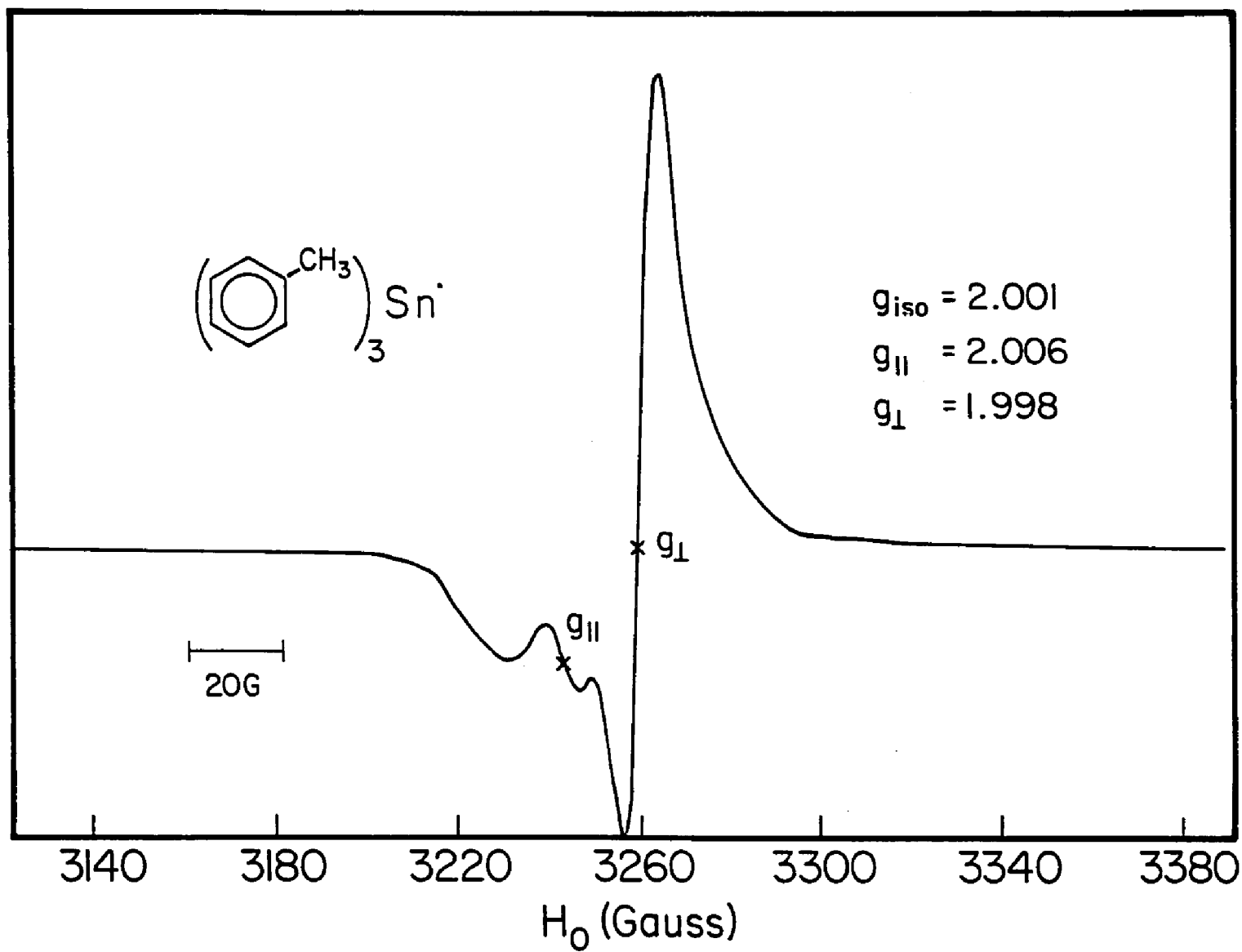
Signal E which is observed at 3971 G is sharp and has a first-derivative line shape with a line-width of 60G. This signal is assigned as the A_{\perp} or A_{xy} in an analogous manner to the triphenyltin radical. Signal F, at 4166 G, is broad and has an absorption line shape with a line-width of 25 G (half-width at half-height). This signal is assigned as the A_{\parallel} or A_z hyperfine coupling. The isotropic and anisotropic hyperfine splittings are listed in table 2. These results are now reported for the first time.

Signals A and B in figure 13 are assigned to the anisotropic g_{\perp} and g_{\parallel} respectively in a similar manner to that of triphenyltin radical. The g values (perpendicular

Figure 13 - The ESR spectra of the central signal at $g = 2$
of $(o\text{-CH}_3\text{-C}_6\text{H}_4)_3\text{}^{119}\text{Sn}$ in 2-MTHF at 93 K.

$$A = g_{\perp}$$

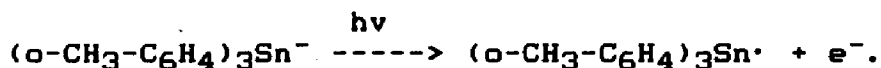
$$B = g_{\parallel}$$



and parallel) have been determined and their values are listed in table 2.

The ESR signal of the triorthotolytin radical is light independent. The irradiation time required to generate sufficient triorthotolytin radicals to obtain a signal to noise ratio of 6:1 is about 7 - 10 minutes. The light independent behavior of the triorthotolytin radical was identical to that of triphenyltin radical.

Warming of the trapped radical from 93°K to 103°K, slightly above the melting point of the matrix, caused the signal intensity to decrease to zero. On recooling to 93°K, the signal did not return until the sample was irradiated again. These results are consistent with a mechanism which assumes the generation of triorthotolytin radical by the photo-oxidation of triorthotolytin anion according to the following reaction:



3. Hyperfine Splittings and g-Factor Determination

ESR data of triorthotolytin radical are listed in table 2. The isotropic and anisotropic hyperfine splittings were calculated from the high-field signals and signal D in an identical manner to that of the triphenyltin radical.

From the analyses of signals E and F in figure 12B, the field associated with the first and second signals are 3971 G and 4166 G, respectively. The field at the central signal D is estimated to be 3265 G. Applying these data in equations (35-37) in section II, the isotropic and anisotropic hyperfine coupling constants are:

$$a_{iso} = 2058 \text{ G}$$

$$a_{||} = 493 \text{ G}$$

$$A_{||} = 2551 \text{ G}$$

$$A_{\perp} = 1811 \text{ G}$$

The positions of the magnetic resonance signals were calculated in similar manner to the triphenyltin radical. The calculated line positions were in good agreement with the observed values as shown in table 4.

4. Ultraviolet (UV) Degradation

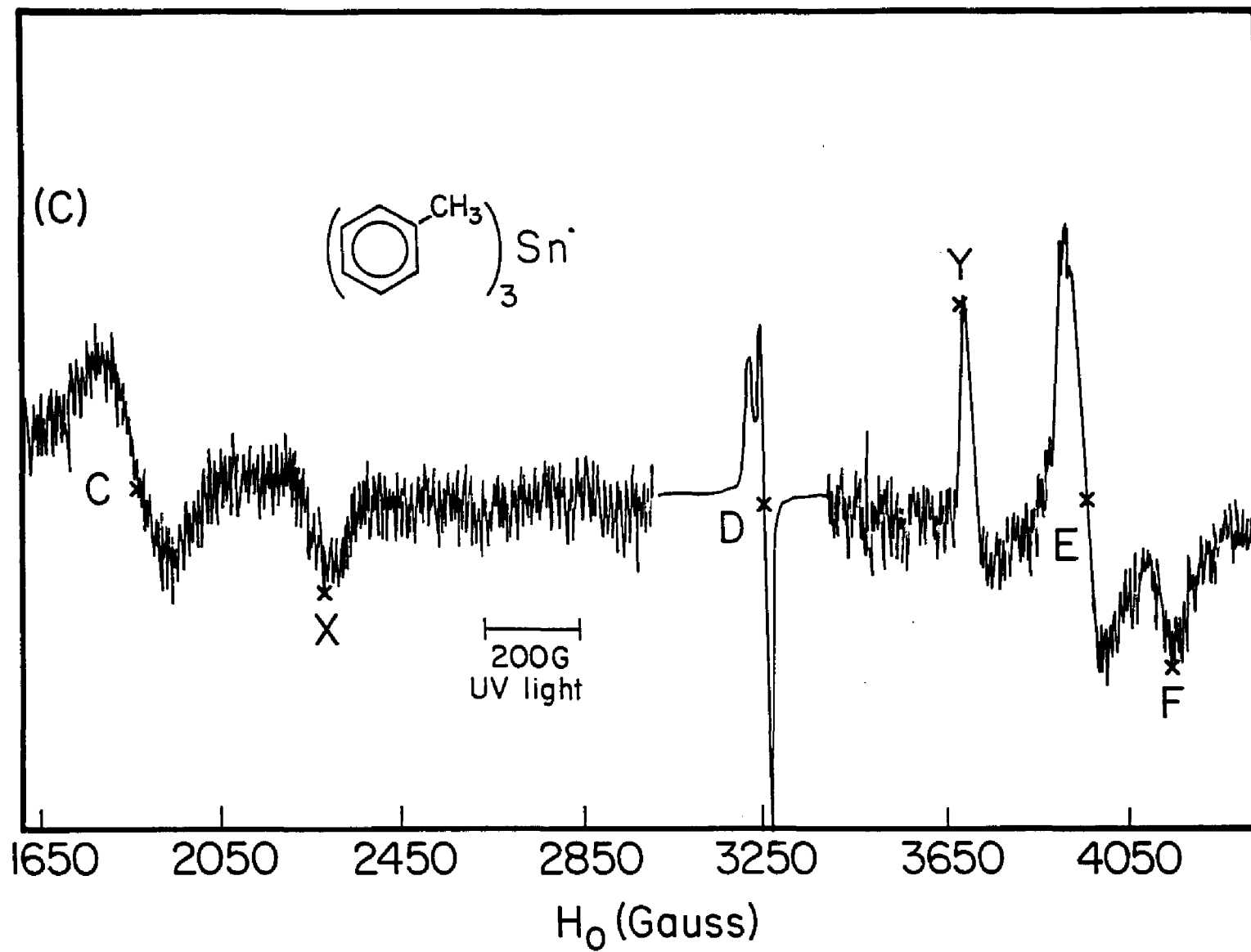
The generation of triorthotolytin radicals has been observed using unfiltered UV light. But the spectral analyses were ambiguous and the accuracy was poor.

Figure 12C shows the ESR spectrum of the tri-orthotolytin radical in 2-MTHF using unfiltered UV light at 93 K. The spectra were identical in line shape and line position with the results observed in figure 12B. The spectrum has a Gaussian line shape and consists of six main features, signals: C, D, E, F, X and Y.

Signals C, E and F in figure 12B were identical in line shape and line position to those observed in figure 12C. Yet, in figure 12C two extra satellites are observed. At low-field, signal X (2265 G) has a first derivative Gaussian line shape and is about 1000 G from the central signal D ($g=2$). Signal Y, at high-field, is observed at 3700 G and is about 450 G from the central signal D. Signals X and Y are unsymmetrically placed about the central signal D. These results are consistent with a model which assumes UV degradation of triaryltin radicals.

Signal D in figure 12C was different from the one in 12B in line shape and in intensity. This is probably due to the UV degradation of 2-MTHF. These results show explicitly the simultaneous production of undetermined radical species. The use of unfiltered ultraviolet radiation as a method of radical generation will complicate the identification of the radical and, therefore, will complicate the spectral analyses.

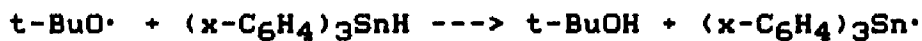
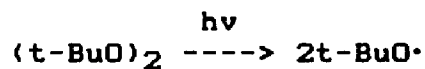
Figure 12C - The ESR spectra of UV irradiated
(o-CH₃-C₆H₄)₃¹¹⁹Sn· in 2-MTHF at 93 K.



D - t-Butyl Peroxide

1. Radical Generation

Following the methods of Lehnig (7), triaryltin radicals were generated in the cavity of the spectrometer by the UV irradiation of di-t-butyl peroxide with the corresponding hydride dissolved in n-pentane according to the following reaction mechanism:



where x (H-, o-CH₃, and p-CH₃).

2. ESR Spectra

Low temperature experiments were performed at 93 K. The radical generated in this manner from triphenyltin hydride gave only a broad signal (18 G peak-to-peak width). No hyperfine splitting was observed. The g value of this signal was found to be 1.995.

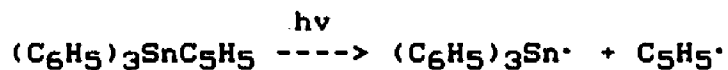
The radical generated from trisorthotolytin hydride gave a broad signal (12G peak-to-peak width). No hyperfine splitting was observed. The g value was found to be 2.005.

The radical generated from trisparatolytin hydride gave a broad signal (10 G peak-to-peak width). No hyperfine splitting was observed. The g value appeared to be 2.004

E - Cyclopentadienyl

1. Radical Generation

Triphenyltin radicals were generated in the cavity of the spectrometer by the UV irradiation of triphenyltin cyclopentadienyl in a 2-MTHF glass according to the following reaction mechanism (12):



2. ESR Spectra

Low temperature experiments were performed at 93 K, using a 2-MTHF filter in place of the UV (pyrex) filter. The radical generated gave only a broad signal (16 G peak-to-peak width). No hyperfine splitting was observed. The g value was found to be 1.996. In the absence of the 2-MTHF filter, UV irradiation produced numerous signals about g=2.

V. DISCUSSION

The observed ESR spectra of isotopically enriched triphenyltin, triorthotolyltin and triparatolyltin, were unsymmetrical and featured a broad signal in the low-field region. The low-field signal suggests that it may contain unresolved structure. The observed down-field signal was found to be bracketed by calculated value when experimental temperature were varied between 93° K and 4° K, the broadened signal did not change line width or line positions. These results indicate that the broadened line is most probably not the result of a kinetic process. It may prove necessary to include second and third order effects in the Breit-Rabi equation to describe these spectral features.

The pyramidal structure for the triaryltin radicals investigated in this study can be rationalized in terms of the electronegativity arguments of Pauling (53) and Morehouse (1). The reported bond angles are calculated from the observed hyperfine splitting. The calculation assumes that the bonding orbitals are "S" and "P" hybrids with no "D" contribution. The electronegativity

of C is 2.5 and that of Sn is 2.0 on the Pauling scale (55). The polarity of the tin-carbon bond is toward the carbon. In aryltin radicals, the non-bonding tin orbital which contains the unpaired electron will have more charge density than the bonding tin orbitals. Thus, the total "S" electron charge density on tin is increased by the "S" character of the unshared orbital. This would result in weakened tin-carbon bonds relative to carbon-carbon bonds and lead to a pyramidal structure.

Triaryltin radical is expected to have C_{3v} symmetry based on the unsymmetrical spectra, large hyperfine coupling and out-of-plane angle. The high "P" character makes it unlikely that the radical has $R_4Sn^{\cdot -}$ instead of R_3Sn^{\cdot} (3), where R = phenyl.

The calculated values for the hyperfine splittings are based on a model which assumes C_{3v} symmetry, (4). They are in good agreement with the observed spectra. It is reasonable to assume that "D" orbitals probably do not participate for two reasons. First, these orbitals do not transform under C_{3v} symmetry as A_2 (54, 4) and second, there is relatively little variation in the magnitude of the g-factor. Variations in the

pyramidal structure of the aryltin radicals investigated in this study can be explained in terms of a positive inductive effect and in terms of steric effects. The methyl substituent in the para-tolyl compound should donate electrons to the phenyl group through induction and hyperconjugation. This type of electron donation, known as the inductive effect, should reduce the electronegativity difference of the tin-carbon bond and thereby decrease the "S" character of the unshared electron. Thus, the para-tolyl radical should be less pyramidal than the parent phenyl radical.

The ortho-tolyl radical is calculated to have a deeper pyramidal structure than the parent phenyl radical. Although, the inductive effect in this radical should be the same as in the p-tolyl radicals, steric hindrances offset the inductive effect. Steric factors, caused by the methyl groups, may lead to angular variation of the phenyl groups. These angular variations will be minimized by increasing the hybrid orbital contribution, which in turn increases the "S" character of the unpaired electron. The increased "S" character is consistent with a deeper pyramidal structure.

The ESR spectra of the visible light irradiated triphenyltin, triparatolytin and triorthotolytin radical have Gaussian line shapes and as described earlier, consist of four main features. In these compounds the $g = 2$ signals are dramatically changed by UV irradiation. In addition, under UV irradiation two extra features are observed for triparatolytin and triorthotolytin. These results are consistent with a model which assumes UV degradation of triparatolytin and triorthotolytin radicals and the simultaneous production of undertermined radical species. The use of unfiltered UV radiation as a method of radical generation will complicate the identification of the radical and, therefore, will complicate the spectral analyses.

This observation is especially important when considering alternate methods of aryltin radical generation which have been reported in the literature. Of particular concern are: (a) methods which use UV photo-chemical production of t-butyl peroxide radicals to abstract protons from tin hydrides in solution, (3, 7), (b) the UV degradation of aryltin cyclopentadienyl to aryltin radical and cyclopentadienyl radical, (12). It is clear that undetermined radical species may be obtained in each case, and therefore yield inaccurate data.

APPENDIX A

I. Computer program for theoretical calculations of triaryltin compounds.

A computer program was written to compute coupling constants, "S" character, "P" character, hybridization, ligand-tin-ligand bond angles and out-of-plane bond angles for aryltin radicals of C_{3v} symmetry. The program uses equations (29-37) section II, the position of the satellite line and the observed field position of the central line. This program was designed for use with a color monitor, or a black and white monitor.

Input Statement

- > The field position of the central line H_0 .
- > The field position of the high-field satellite H_{1z} .
- > The field position of the high-field satellite H_{1xy} .
- > The theoretical hyperfine splitting A .
- > The theoretical anisotropic hyperfine splitting B_z .

Output Statement

- > Hyperfine splitting A_z .
- > Hyperfine splitting A_{xy} .
- > Isotropic hyperfine splitting.

- > Anisotropic hyperfine splitting.
- > S-Character.
- > P-Character.
- > Total spin density.
- > Hybridization.
- > Interbond angle (ligand-metal-ligand).
- > Out of plane angle.

Program Listing:

```
>10  color 0,2,1
>20  CLS:  KEY  OFF  :PRINT  "THEORETICAL  CALCULATION  OF
      TRIARYLTIN  COMPOUNDS"
>30  PRINT  "PROGRAM  WRITTEN  BY  SOBHY  EL-HEFNAWI,
      3/86":PRINT
>40  PRINT  "THE  RADICAL'S  NAME  IS  ":PRINT
>50  INPUT  "ENTER  THE  FIELD  POSITION  OF  THE  CENTRAL  LINE
      HO:  ",HO
>60  INPUT  "ENTER  THE  FIELD  POSITION  OF  THE  HIGH-FIELD
      SATELLITE  HLZ:  ",HL1
>70  INPUT  "ENTER  THE  FIELD  POSITION  OF  THE  HIGH-FIELD
      SATELLITE  HLXY:  ",HL2
>80  INPUT  "ENTER  THEORETICAL  HYPERFINE  SPLITTING  A:  ",A
>90  INPUT  "ENTER  THEORETICAL  ANISOTROPIC  HYPERFINE
      SPLITTING  BZ:  ",BZ
>100  C1=HL1-HO:C2=HL2-HO
```

```
>110 F1=2*HO
>120 E1=F1*C1:E2=F1*C2
>130 R1=F1-HL1:R2=F1-HL2
>140 AZ=E1/R1:AXY=E2/R2
>150 D=1/3*(AZ+2*AXY)
>160 E=2/3*(AZ-AXY)
>170 PRINT "HYPERFINE SPLITTING (AZ) = "AZ
>180 PRINT "HYPERFINE SPLITTING (AXY) = "AXY
>190 PRINT "ISOTROPIC HYPERFINE SPLITTING = "D
>200 PRINT "ANISOTROPIC HYPERFINE SPLITTING = "E
>210 F=D/A
>220 G=E/BZ
>230 I=F+G
>240 H=G/F
>250 PRINT "S-CHARACTER="F
>260 PRINT "P-CHARACTER=" G
>270 PRINT "TOTAL SPIN DENSITY=" I
>280 PRINT "HYPERDIZATION = "H
>290 X=1.5/(2*H+3)-.5
>300 PHI=1.570796-ATN(X/SQR(1-X*X))
>310 Y=1/3*(1+2*COS (PHI))
>320 THETA=1.570796-ATN(SQR(Y)/SQR(1-Y))
>330 PRINT "INTERBOND ANGLE (LIGAND-METAL-LIGAND)="
      PHI*180/3.141593
>340 PRINT "ANGLE BETWEEN SYMMETRY AXIS AND LIGAND BOND =
      " THETA*180/3.141593
```

```
>350 PTINT "OUT-OF-PLANE ANGLE = "90-THETA*180/3.141593
>360 V$=INKEY:IF V$=""THEN 360
>370 INPUT "DO YOU WANT TO TRY AGAIN (Y/N)"; A$:IF A$="Y"
      THEN CLS : GOTO 40
>380 COLOR 7,0,0:CLS:KEY ON:END
```

EXAMPLE

Input Statement

The field position of the central line $H_0=3272$ G
The field position of the high-field satellite $H_{1z}=4117$ G
The field position of the high-field satellite $H_{1xy}=3913$ G
The theoretical hyperfine splitting $A= 15600$ G
The theoretical anisotropic hyperfine splitting $B_z=520$ G

Output Statement

Hyperfine splitting $A_z=2280$ G
Hyperfine splitting $A_{xy}=1594$ G
Isotropic hyperfine splitting= 1823
Anisotropic hyperfine splitting= 457 G
S-Character= 0.117
P-Character= 0.879
Total spin density= 0.996
Hybridization= 7.52
Interbond angle (ligand-metal-ligand)= 114.6
Out of plane angle= 13.6

II. Computer program for theoretical calculation of low-field satellite positions.

This computer program was written to calculate the position of the low-field signals. The program uses equations 36-37, the hyperfine splitting and the observed field position of the central line.

Input Statement

- > The field position of the central line H_0 .
- > The calculated hyperfine splitting A.

Output Statement

- > The low-field satellite position.

Program Listing:

```
>10 Color 0,2,1
>20 CLS: KEY OFF :PRINT "THERETICAL CALCULATION OF
LOW-FIELD SATELLITE"
>30 PRINT "PROGRAM WRITTEN BY SOBHY EL-HEFNAWI,3/86":
PRINT
>40 PRINT :INPUT "ENTER THE FIELD POSITION OF THE
CENTRAL-LINE HO: ",HO
```

```
>50 PRINT INPUT "ENTER THE CALCULATED HYPERFINE  
SPLITTING A: ",A  
>60 F=2*H0  
>70 P=A-H0  
>80 Q=A-F  
>90 K=F*P  
>100 HK=K/Q  
>110 PRINT "LOW-FIELD SATELLITE= "HK  
>120 V$=INKEY$: IF V$="" THEN 120  
>130 INPUT "DO YOU WANT TO CALCULATE ANOTHER ONE (Y/N)";  
A$:IF A$="Y" THEN CLS :GOTO 40  
>140 COLOR 7,0,0:CLS:KEY ON :END
```

EXAMPLE

Input Statement

The field position of the central line $H_0=3272$ G

The calculated hyperfine splitting $A=1594$ G

Output statement

The low-field satellite position= 2218 G

III. Computer program for theoretical calculation of hyperfine splitting.

This computer program was written to calculate the parallel or perpendicular hyperfine splitting. The program uses equations 36-37, the field position of the high-field satellite and the observed field position of the central line.

Input Statement

- > The field position of the central line H_0 .
- > The field position of the high-field satellite H_L .

Output Statement

- > The hyperfine splitting A .

Program Listing:

```
>10  Color 0,2,1
>20  CLS:  KEY  OFF  :PRINT  "THERETICAL  CALCULATION  OF
      HYPERFINE  SPLITTING"
>30  PRINT  "PROGRAM  WRITTEN  BY  SOBHY  EL-HEFNAWI,3/86":
      PRINT
>40  PRINT  :INPUT  "ENTER  THE  FIELD  POSITION  OF  THE
      CENTRAL-LINE  HO:  ",HO
```

```
>50 PRINT :INPUT "ENTER THE FIELD POSITION OF THE  
HIGH-FIELD SATELLITE HL: ",HL  
>60 C=HL-HO  
>70 F=2*HO  
>80 E=F*C  
>90 R=F-HL  
>100 A=E/R  
>110 PRINT :PRINT "HYPERFINE SPLITTING= "A  
>120 V$=INKEY$: IF V$=""THEN 120  
>130 INPUT "DO YOU WANT TO CALCULATE ANOTHER ONE (Y/N)";  
A$:IF A$="Y" THEN CLS :GOTO 40  
>140 COLOR 7,0,0:CLS:KEY ON :END
```

EXAMPLE

Input Statement

The field position of the central line $H_0=3272$ G

The field position of the high-field satellite $H_1=3913$ G

Output Statement

The hyperfine splitting =1594 G

BIBLIOGRAPHY

1. Morehouse, R. N.; Christiansen, J. J.; Gordy, W. J. Chem. Phys. **1966**, 45, 1751.
2. Lehnig, M.; Doren, K. J. Organomet. Chem. **1981**, 210, 331
3. Fieldhouse, S. A.; Lyons, A. R.; Starkie, H. C.; Symons, M. C. R. J. Chem. Dalton. Trans. **1974**, 18, 1966.
4. Berclaz, T.; Geoffroy, M. Chem. Phys. Lett. **1977**, 52, 606.
5. King, B. A.; Bramwell, F. B. J. Inorg. Nucl. Chem. **1981**, 43, 1479.
6. Lehnig, M.; Neumann, W. P.; Apoussids, Th. Chem. Phys Lett. **1983**, 100, 189.
7. Lehnig, M.; Neumann, W. P.; Apoussids, Th.; Bauschhaus, H. U. Bull. Soc. Chim. Belg. **1980**, 89, 907
8. El-Farargy, A. F.; Lehnig, M.; Neumann, W. P. Chem. Ber. **1982**, 115, 2782.
9. Griffiths, V. S; Derwish, G. A. W. J. Mol. Spec. **1960**, 2, 148
10. Eng, G.; Dillard, C. R. Inorg. Chimica. Acta. **1978**, 31, 227.
11. Hamid, M. A. Can. J. Chem. **1973**, 51, 2759.
12. Davies, A. G. Pure & Appl. Chem. **1982**, 54, 1, 23
13. Schmidt, U.; Kabrtzke, K.; Markan, K.; Neumann, W. P. Chem. Ber. **1965**, 98, 3827.
14. Geoffroy, M.; Hammons, J. H. J. Chem. Educ. **1981**, 58, 389.
15. Drago, R. S. "Physical Methods in Chemistry" W. B. Saunders Co., Phil. PA, 1977.

16. Ayscough, P. B.; "Electron Spin Resonance in Chemistry" Methuen and Co. LTD., London, 1967.
17. Atkins, P. W.; Symons, M. R. "The Structure of Inorganic Radicals" Elsevier, Amsterdam, 1967.
18. Horsfield, A; Morton, J. R.; Whiffen, D. H. Mol. Phys. 1961, 4, 475.
19. Breit, G.; Rabi, I. Phys. Rev. 1931, 38, 2082.
20. Hudson, A; Lappert, M.; Lednor, P. J. C. S. Dalton 1976, 2370.
21. Wertz, J.; Bolton, J. "Electron Spin Resonance" Chapman and Hall, N.Y. 1986.
22. Morton, J. R.; Preston, K. F. J. Mag. Res. 1978, 30, 577.
23. Barnes, R. G.; Smith, V. Phys. Rev. 1954, 93, 95.
24. Froese, C. J. Chem. Phys. 1966, 45, 1417.
25. Mackey, J. H.; Wood, D. E. J. Chem. Phys. 1970, 52, 4914.
26. Biltz; Hall; Blanchard. "Laboratory Methods of Inorganic Chemistry", 2nd Ed.; John Wiley and Son, NY 1928; p 20.
27. Whaley, T. P. Inorganic Synthesis, 1954, 4, 119.
28. Whaley, T. P. Inorganic Synthesis, 1957, 5, 71.
29. William, L. J. "The synthesis and Characterization of Inorganic Compounds" p 475 - 478.
30. Chambers, R. F.; Scherer, P. C. J. Am. Chem. Soc. 1926, 48, 1054.
31. Weiss, R. W. "Organometallic Compounds-Methods of Synthesis, Physical Constants and Chemical Reactions", 2nd Ed.; Springer Verlag, NY 1967.
32. Kozeschkow, K. A.; Nadj, M. M.; Alexandrow, A. P. Chem. Ber. 1934, 67, 1348.

33. Grignard, V.; Courtot, C. Compt. Rend. 1914, 158, 1763.
34. Gillman, H.; Gist, L. A. J. Org. Chem. 1957, 22, 250.
35. Fritz, H. P.; Kreiter, C. G. J. Organomet. Chem. 1964, 1, 323.
36. Kuivila, H.; Beumel, O. F. J. Am. Chem. Soc. 1961, 83, 1246.
37. Kula, M.; Amberger, E.; Fritz, H. P.; Kreiter, C. G. Chem. Ber. 1963, 96, 3270.
38. Sawyer, A. "Organometallic Compounds" Marcel Dekker Inc. 1972, NY. Vol. 3, Chap. 13.
39. Krause, E.; Becker, R. Chem. Ber. 1920, 53, 173.
40. Lorenz, D. H.; Shapiro, P.; Stern, A.; Becker, E. J. Org. Chem. 1963, 28, 2332.
41. Stern, A.; Becker, E. L. J. Org. Chem. 1964, 29, 3221.
42. Bramwell, F. B.; Gendell, J. J. Chem. Phys. 1970, 52, 5656.
43. Ward, L. R. J. Am. Chem. Soc. 1961, 83, 296.
44. Tuttle, T. R.; Weissman, S. I. J. Am. Chem. Soc. 1958, 80, 5342.
45. Paul, E. D.; Lipkin, D.; Weissman, S. I. J. Am. Chem. Soc. 1956, 78, 116.
46. Bolton, J. R.; Fraenkel, G. K. J. Chem. Phys. 1964, 40, 3307.
47. Cox, R. H.; Janzen, E. G.; Harrison, W.P. J. Mag. Res. 1971, 4, 274.
48. Blake, D.; Coates, G. E.; Tate, J. M. J. Chem. Soc. 1961, 618.
49. Tamborski, C.; Ford, F. E.; Lehn, W. L.; Moore, G. E. J. Org. Chem. 1962, 27, 619.

50. Gillman, H.; Marrs, O. L.; Sims, S. J. Org. Chem. 1962, 27, 4232.
51. Tamborski, C.; Ford, F. E.; Soloski, E. J. J. Org. Chem. 1963, 28, 181.
52. Linschitz, H.; Perry, M. G.; Schweitzer, D. J. Am. Chem. Soc. 1954, 76, 5833.
53. Pauling, L. J. Chem. Phys. 1969, 51, 2767.
54. Booth, R. J.; Fieldhouse, S. A.; Starkie, H. C.; Symons, M. C. R. J. Chem. Dalton. 1976, 1506.
55. Allred, A. L. J. Inorg. Nucl. Chem. 1961, 17, 215.